AFRL-RX-WP-JA-2018-0320

FROM HIGH ENTROPY ALLOYS TO COMPLEX CONCENTRATED ALLOYS (POSTPRINT)

S. Gorsse
CNRS, University Bordeaux

J.P. Couzinié
Université Paris Est

D. Miracle
AFRL/RX

30 AUGUST 2018
Interim Report

(STINFO COPY)

AIR FORCE RESEARCH LABORATORY
MATERIALS AND MANUFACTURING DIRECTORATE
WRIGHT-PATTERSON AIR FORCE BASE, OH 45433-7750
AIR FORCE MATERIEL COMMAND
UNITED STATES AIR FORCE

REPORT DOCUMENTATION PAGE

Form Approved
OMB No. 0704-0188

1. REPORT DATE *(DD-MM-YY)*	2. REPORT TYPE	3. DATES COVERED *(From - To)*
30 August 2018	Interim	19 March 2014 – 30 July 2018

4. TITLE AND SUBTITLE
FROM HIGH ENTROPY ALLOYS TO COMPLEX CONCENTRATED ALLOYS (POSTPRINT)

5a. CONTRACT NUMBER
IN-HOUSE

5b. GRANT NUMBER

5c. PROGRAM ELEMENT NUMBER

6. AUTHOR(S)
1) S. Gorsse – CNRS
2) J.P. Couzinié – Université Paris Est
(Continued on page 2)

5d. PROJECT NUMBER

5e. TASK NUMBER

5f. WORK UNIT NUMBER
X0W6

7. PERFORMING ORGANIZATION NAME(S) AND ADDRESS(ES)
1) CNRS, University Bordeaux ICMCB, UPR 9048, F-33600 Pessac, France
2) Université Paris Est ICMPE (UMR 7182), CNRS, UPEC, Thiais, France
(Continued on page 2)

8. PERFORMING ORGANIZATION REPORT NUMBER

9. SPONSORING/MONITORING AGENCY NAME(S) AND ADDRESS(ES)
Air Force Research Laboratory
Materials and Manufacturing Directorate
Wright-Patterson Air Force Base, OH 45433-7750
Air Force Materiel Command
United States Air Force

10. SPONSORING/MONITORING AGENCY ACRONYM(S)
AFRL/RXCM

11. SPONSORING/MONITORING AGENCY REPORT NUMBER(S)
AFRL-RX-WP-JA-2018-0320

12. DISTRIBUTION/AVAILABILITY STATEMENT
DISTRIBUTION STATEMENT A. Approved for public release: distribution is unlimited.

13. SUPPLEMENTARY NOTES
PA Case Number: 88ABW-2018-4345; Clearance Date: 30 Aug 2018. This document contains color. Journal article published in Comptes Rendus Physique, Vol. 19, No. 8, 8 Dec 2018. © 2018 Académie des Sciences. The U.S. Government is joint author of the work and has the right to use, modify, reproduce, release, perform, display, or disclose the work.
The final publication is available at https://doi.org/10.1016/j.crhy.2018.09.004

14. ABSTRACT ***(Maximum 200 words)***
High-entropy alloys (HEAs) and related concept of complex concentrated alloys (CCAs) expand the diversity of the materials world and inspire new ideas and approaches for the design of materials with an attractive combination of properties. Here, we present a critical review of the field with the intent of summarizing the principles underlying their birth and growth. We highlight the major accomplishments and progresses over the last 14 years, especially in the discovery of new microstructures and mechanical properties. Finally, we outline the main challenges and provide guidance for future works.

15. SUBJECT TERMS
High entropy alloys; Alloy design; Microstructures; Combinatorial metallurgy; Mechanical properties; Computational thermodynamic

16. SECURITY CLASSIFICATION OF:			17. LIMITATION OF ABSTRACT:	18. NUMBER OF PAGES	19a. NAME OF RESPONSIBLE PERSON (Monitor)
a. REPORT	b. ABSTRACT	c. THIS PAGE			Bill Song
Unclassified	Unclassified	Unclassified	SAR	19	19b. TELEPHONE NUMBER *(Include Area Code)* (937) 255-1351

REPORT DOCUMENTATION PAGE Cont'd

6. AUTHOR(S)

3) D. Miracle – AFRL/RX

7. PERFORMING ORGANIZATION NAME(S) AND ADDRESS(ES)

3) AFRL/RX
Wright-Patterson AFB, OH 45433

C. R. Physique 19 (2018) 721–736

Contents lists available at ScienceDirect

Comptes Rendus Physique

www.sciencedirect.com

New trends in metallic alloys / Alliages métalliques : nouvelles tendances

From high-entropy alloys to complex concentrated alloys

Des alliages à haute entropie aux alliages concentrés complexes

Stéphane Gorsse [a,b,*], Jean-Philippe Couzinié [c], Daniel B. Miracle [d]

[a] *CNRS, ICMCB (UMR 5026), Université de Bordeaux, 33600 Pessac, France*
[b] *Bordeaux INP, ENSCBP, 33600 Pessac, France*
[c] *Université Paris Est, ICMPE (UMR 7182), CNRS, UPEC, 94320 Thiais, France*
[d] *Air Force Research Laboratory, Materials and Manufacturing Directorate, Wright-Patterson AFB, OH 45433, USA*

ARTICLE INFO

Article history:
Available online 15 October 2018

Keywords:
High entropy alloys
Alloy design
Microstructures
Combinatorial metallurgy
Mechanical properties
Computational thermodynamic

Mots-clés :
Alliages à haute entropie
Conception d'alliages
Microstructures
Métallurgie combinatoire
Propriétés mécaniques
Thermodynamique computationnelle

ABSTRACT

High-entropy alloys (HEAs) and related concept of complex concentrated alloys (CCAs) expand the diversity of the materials world and inspire new ideas and approaches for the design of materials with an attractive combination of properties. Here, we present a critical review of the field with the intent of summarizing the principles underlying their birth and growth. We highlight the major accomplishments and progresses over the last 14 years, especially in the discovery of new microstructures and mechanical properties. Finally, we outline the main challenges and provide guidance for future works.

RÉSUMÉ

Les alliages à haute entropie (HEA) et le concept associé d'alliages concentrés complexes (CCA) élargissent la diversité du monde des matériaux et inspirent de nouvelles idées et approches pour la conception de matériaux présentant une combinaison attrayante de propriétés. Nous présentons ici une revue critique du domaine dans le but de résumer les principes qui sous-tendent leur naissance et leur développement. Nous mettons en évidence les principaux accomplissements et les progrès réalisés au cours des 14 dernières années, en particulier la découverte de nouvelles microstructures et propriétés mécaniques. Enfin, nous décrivons les principaux défis et suggérons des orientations pour les travaux futurs.

* Corresponding author at: ICMCB (UMR 5026), Bordeaux INP, 33600 Pessac, France.
E-mail address: stephane.gorsse@icmcb.cnrs.fr (S. Gorsse).

https://doi.org/10.1016/j.crhy.2018.09.004

1. Introduction

5000 years of metallurgy have tremendously expanded the diversity of the materials universe, stimulated by the discovery of alloying – the strengthening of one base element by light additions of others – at the bronze age, and the ways to manipulate the microstructure when it was realized in the 1990s that alloy properties depend on scale. Since 2004, a new alloy design strategy that was originally motivated by the exploration of the uncharted central regions of multi-component phase diagrams, powers an explosive growth of new multi-element alloy bases, high-entropy alloys (HEAs), which goes far beyond the traditional approach to develop structural metallic alloys. The initiative taken 14 years ago at the National Tsing Hua University (Taiwan) and Oxford University (UK) has spawned great efforts in many universities and national laboratories in China, France, Germany, India, Japan, South Korea, and the United States. HEAs are now ready to usher in a new era of complexity, offering new degrees of freedom to create useful new materials with better performance, challenging the materials researcher's practices and scientific knowledge, and boosting the development of new approaches for their study and design. The science and engineering of HEAs has now reached a level at which it can disruptively modify the materials designer methods and make technological impact.

In this paper, we step back over the rapid development of HEAs to discuss their principles and the new concepts they introduce, their microstructures and properties, their design strategies, and the ways to accelerate their development with computationally based approaches. The first section puts the birth of HEAs in the context of materials history to highlight how their design principle goes beyond the single idea developed many millennia in the past to now create vast numbers of new metallic materials. In section 3, we summarize the features established in the first generation of HEAs to emphasize the unusual microstructures and properties that have been already produced. The final section forges ahead in the development of refractory complex concentrated alloys (RCCAs), integrating predictive modeling and computational high throughput-based design approach that supplant the traditional process of trial-and-error empiricism.

2. Basic principles and major concepts

Before the birth of the high-entropy alloy (HEA) field, humanity has used a single concept to develop metallic alloys. Since this is the only approach we have ever used, it is easy to forget that there may be other concepts that may consequently produce different properties than those obtained to date. In this opening section, the conventional approach for conceiving and developing metallic alloys is described in an historical context. By contrast, the new concepts supporting the HEA approach are introduced. The evolution of thought over the first 14 years of the HEA field is summarized as a background for the major themes developed in subsequent sections of this paper.

2.1. Lightly alloyed base elements – a brief history and the problem statement

Over 5,000 years ago, the first alloy developer in human pre-history produced bronze by mixing a small amount of tin into copper, and mankind has used the same approach for devising new alloys ever since. Specifically, a base element with attractive properties is used as a starting point, and relatively small levels of alloying elements are added to improve the balance of properties. Iron began to replace bronze around 1200 BCE, and 600 years later steel was produced by controlling small carbon additions to the iron base. The last stable element (Hf) was discovered in 1922, and by 1950 humanity had exploited all of the metallic base elements with potential for major commercial and industrial use, using the same alloying approach first conceived almost 5,000 years earlier. Titanium was the last metallic element exploited as a major alloy base.

After the initial exploitation of all attractive metallic base elements, alloying efforts have become more sophisticated. One characteristic of this growing refinement is that a single base element has often evolved to give several distinct alloy systems. Aluminum alloys are a case in point: 2xxx series aluminum alloys use Cu as the main alloying element; 3xxx alloys use Mn as the defining alloy element; 4xxx series Al alloys primarily use Si; and 5xxx series alloys all contain Mg as the main alloying element. Further, many alloy systems now have controlled additions of two primary alloying elements. Using aluminum alloys as an example once again, the 6xxx series uses relatively small additions of both Mg and Si, while 7xxx Al alloys have both Zn and Mg. Other well-known alloys with two primary elemental additions include Ti-6Al-4V (wt. %) and austenitic stainless steels such as Fe–18Cr–8Ni (wt. %). Some alloys, such as Cr–Mo steels, have intentional additions of three or more elements, and other alloys (such as 'superalloys') can have as many as 12 carefully controlled elemental additions. As a final trait of the intricacy involved with conventional alloy development, the concentrations of added elements are specified to tenths or even hundredths of a percent. In spite of this impressive sophistication, conventional alloy design still uses the same basic approach that was used to develop bronze over 5,000 years ago. Even with multiple elemental additions, all alloys still have a clearly identifiable, dominant base element. To illustrate this point, a large number of conventional commercial or industrial alloys have at least 90% by weight of the base element, most have 80% by weight, and the base element accounts for at least 50% by weight for all but a small number of alloys in two alloy families (Fig. 1).

This sophisticated, conventional alloying approach has been very successful, and has produced alloys with spectacular blends of properties. It has formed the foundations of human civilizations, from the bronze age to the industrial age and to the 21st century. However, there are indications that this approach may be reaching a limit and may no longer provide alloys and properties needed for new technological challenges. There are no new stable metallic elements to give new elemental alloy bases. In a growing number of cases, efforts to develop alloys with significantly different (and highly impactful)

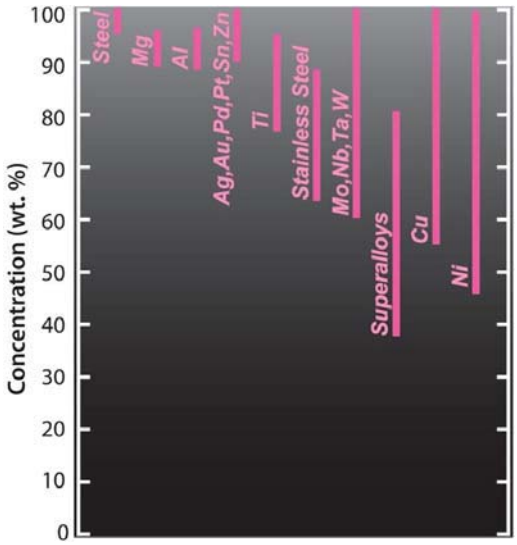

Fig. 1. The ranges of base element concentrations for commercially or industrially important metallic alloy families. All of the alloys in many base element families have at least 90% by weight of the base element, including steels and alloys based on Al, Mg, Ag, Au, Pd, Pt, Sn or Zn. Most alloys have at least 80% by weight of the base element, and all but a small number of superalloys and austenitic nickel alloys have more than 50% by weight of the base element. Data taken from [1].

properties have ended in failure after decades of intense international study. This includes efforts to increase the maximum use temperature of nickel-based superalloys, or to reduce reliance on strategic elements, or to produce new low-cost or low-density materials. These failures have fueled concern that perhaps a fundamentally new idea is needed to develop alloys with significantly different properties than those that have been produced by the historical, lightly alloyed base element approach.

2.2. High-entropy alloy concept – major ideas and motivations

The HEA field was launched in 2004 in two separate papers from two different research groups with two different motivations [2,3]. The motivation in one paper was "to investigate the unexplored central region of multicomponent alloy phase space" [2]. By using concentrated blends of several (or many) elements as a new alloy base, this paper established the idea that the central regions of multi-component phase diagrams provided a cosmically vast number of new, unexplored alloy bases. The second study was motivated by the possibility of favoring single-phase solid solution alloys over intermetallic-containing microstructures by controlling the configurational entropy via alloy composition [3]. In this approach, HEAs are defined as alloys with 5 or more principal elements that have concentrations between 5 and 35 atom percent. Together, these papers provide the two distinctive ideas that are the foundation of the HEA field.

The specific combination of principal elements in an HEA gives a new alloy 'base', analogous to the elemental alloy base in the historical alloy approach. The vast number of new alloy bases comes from the vast number of ways that r principal elements can be taken from a palette of n candidates. The equation describing the number of unique combinations of principal elements is

$$C_r^n = \frac{n!}{r!\,(n-r)!}$$

There are 67 stable metallic elements, giving 47,905 ternary alloy bases, 766,480 quaternary bases and a total of over 110 million new alloy bases with 3, 4, 5 or 6 principal elements. This very large number compares with only 67 elemental alloy bases from the same palette of 67 metallic elements (fewer than two dozen elements have an attractive blend of properties that have supported ultimate development for actual use, see Fig. 1). Unlike an elemental alloy base, which gives only one base per element, a combination of r particular elements can give many new alloy bases by changing the concentrations of the r elements. For example, HEAs based on $Al_xCoCrFeNi$ and $Al_xCoCrFeNi_2$ give a base alloy that is dominated by an fcc crystal structure when $x \leq 0.4$, give a base alloy with both bcc and fcc phases when $0.5 \leq x \leq 1$, and give a base alloy dominated by the bcc structure when $x > 1$ (see data in [4–6]).

Finally, like conventional alloys, an HEA 'base' of r principal elements can be further modified by minor additions of other (non-principal) elements. Together, these HEA features give a cosmically vast number of new alloys that are difficult to quantify or conceive.

2.3. Entropy and enthalpy

The motivation to discover and study new solid solution HEAs dominated the field for the first decade. This was embodied by the high entropy hypothesis – that single phase solid solution microstructures might be favored by the independent control of configurational entropy through alloy compositions. As a result, HEAs became essentially synonymous with single-phase solid solution alloys, even though this was not required by any of the HEA definitions. Two major issues emerged with this focus. First, the high entropy hypothesis makes the strong assumption that the constituent element species are randomly distributed on the solid solution (SS) lattice sites so that the entropy (S) can be adequately described by the ideal, Boltzmann configurational entropy

$$S^{\mathrm{SS,ideal}} = -R \sum_i x_i \ln (x_i)$$

where R is the gas constant and x_i is the atom fraction of alloy element i. Contrary to this assumption, thermodynamic analysis of nearly 1200 binary alloys suggests that ideal solutions are uncommon, and that sub-regular solutions (solutions that are far from ideal) account for a clear majority (85%) of binary alloys [4]. Second, the focus on configurational entropy frequently ignored the essential contribution of enthalpy to phase stability and selection. Ultimately, extensive analysis of the data available concluded that the high entropy hypothesis is not supported by experimental and computational results [4,7–9]. Especially, increasing the number of principal elements not only increases entropy, but also changes enthalpy by significantly increasing the number of constituent element pairs, and hence increasing the possibility that at least one pair of atom species may have formation enthalpies that out-compete configurational entropy.

Detailed analysis now shows that entropy and enthalpy both exert an important influence and both need to be considered to accurately predict formation of solid solution and intermetallic phases [4,8]. This is required by long-established thermodynamic concepts (entropy and enthalpy are both specified in the Gibbs energy equation) and may therefore seem rather obvious. Nevertheless, this corrects an earlier apparent bias toward considering enthalpy alone and ignoring entropy. The important role of entropy is now better understood, and the high entropy field has introduced and developed the important idea that entropy can be adjusted (although not independent of enthalpy) by controlling alloy composition.

2.4. HEA families and element selection rules

The early emphasis on single-phase, solid solution HEAs had the unintended consequence of limiting the number of new alloy families that were defined and explored. The CoCrFeMnNi solid solution phase (the so-called ‘Cantor alloy’) was discovered in one of the very first HEA papers [2], and for the next six years the HEA field pursued a nearly singular focus on alloys based on these elements. The Cantor alloy forms the basis of what is now referred to as the 3d transition metal (3d TM) family of HEAs. Alloys in this family include four or more principal elements from a palette of 9 elements (Al, Co, Cr, Cu, Fe, Mn, Ni, Ti, and V) [4,10]. The selection of principal and minor alloying elements in 3d TM alloys has been guided by the motivation to explore compositional effects on microstructure and properties. 3d TM HEAs are an extension of austenitic stainless steels, austenitic nickel alloys and nickel-based superalloys [4,10]. All of these have Fe, Ni and Cr as principal elements, and all have microstructures dominated by the expansion of the austenitic fcc phase field.

The first new family of HEAs was introduced in 2010 [11]. Motivated by the desire to develop high temperature structural alloys with maximum use temperatures above 1000°C, this refractory HEA (RHEA) family initially drew on five refractory metals in Groups 5 and 6 of the periodic table (Mo, Nb, Ta, V, W). The palette of principal elements now used for RHEAs has grown to include nine refractory metals (Cr, Hf, Mo, Nb, Re, Ta, V, W, Zr), two 3d transition metals (Co, Ni) and five compound-forming elements (Al, C, N, Si, Ti) [12]. Soon after the introduction of RHEAs, the intentional design of other alloy families began. The 4f transition metal (4f TM) alloy family was motivated by the desire to form a single-phase hcp solid solution HEA [13–15]. Low density HEAs were pursued to explore new, lightweight structural alloys [16,17], and HEA brasses and bronzes were developed to improve the balance of properties offered by conventional brasses and bronzes [18]. Finally, noble metal HEAs were conceived to reduce material cost relative to conventional alloys based almost entirely on very expensive elements such as Pt or Pd, used in jewelry or catalytic applications [19]. Compared to essentially pure Pd or Pt, these HEAs can reduce cost significantly by adding less expensive noble metal principal elements such as Ag or Ru. The noble metal HEA palette also includes the 3d transition metals Co, Cr, Cu and Ni, offering further potential to reduce alloy cost.

Element selection for these alloy families is based on a rather intuitive approach. For example, principal elements with high melting temperatures (T_m) are selected for RHEAs, low-density elements are used for low density HEAs, and elements with an hcp crystal structure are used to produce single-phase, solid solution HEAs with the hcp crystal structure. Initial efforts already exist to think beyond this obvious first approach. For example, elements with low T_m are also used in RHEAs. The concept supporting the use of these elements is still logical and rather simple, since these low-T_m elements usually form compounds that have high T_m. Al is a common example – it combines with many elements to form a high-melting intermetallic phase. Specifically, NiAl and CoAl melt at higher temperatures than Al, Co or Ni. Similar results are found for Si. A detailed description of a rational, systematic approach to element selection is given for structural metals used at low, intermediate and high temperatures [20]. More radical departures from this intuitive method of element selection have been

recommended [21], and will be enabled by new computational techniques and high-throughput experiments described in Section 4.2 of this review.

HEAs based on oxides, borides, carbides and nitrides are now a well-established area of research [4]. HEAs for functional applications are also being studied [22]. To maintain focus, the present paper emphasizes on metallic HEAs for structural applications and briefly refers to functional properties.

2.5. Expansion of the HEA field – introducing complex, concentrated alloys (CCAs)

As discussed above, thought in the early years of the HEA field was dominated by configurational entropy and the search for single-phase, solid solution alloys. The HEA definition further restricted studies to alloys with 5 or more principal elements, even though interesting results were being obtained in concentrated alloys with only 3 or 4 principal elements. This restriction of thought began to evolve in unproductive ways by excluding new results in new alloy systems based solely on the number of elements used or the number and types of phases formed. This early exclusion seems strange, especially in a field founded on the concept of unbounded expansiveness of alloy compositions and microstructures.

It was concluded that the HEA field is too broad to be adequately described by a single definition or microstructure, and so new terms were introduced to help remove these barriers [23]. These new terms include complex concentrated alloys (CCAs), multi-principal element alloys (MPEAs), or simply 'baseless' alloys. These more inclusive terms retain focus on concentrated alloys that are also compositionally complex and thus have no single, dominant element. Definitions ultimately set boundaries, and so these new terms intentionally avoid specific definitions based on the number or concentration ranges of elements used or the number or types of phases formed. These new terms also have no implications regarding the magnitude or importance of configurational entropy. These new terms include every alloy that satisfies HEA definitions, and they also include many alloys that are excluded by HEA definitions. They thus expand the HEA field by including concentrated ternary and quaternary alloys, by allowing elemental concentrations in excess of 35 atomic percent, and by including single-phase intermetallic alloys and alloys with any number of solid solution and intermetallic phases. Finally, the early years of the HEA field were dominated by studies of metallic alloys for structural applications, but these new terms specifically include non-metallic alloys and alloys developed for functional applications [4]. Complex concentrated alloys (CCAs) are used in the present work to include all alloys in the HEA field, as well as alloys that satisfy the motivation of studying complex, concentrated alloys or the vast number of compositions and microstructures in the central regions of multi-component phase diagrams.

3. Features established in the first-generation HEAs

3.1. Unusual microstructures

A review of the CCA field shows that amorphous, nanocrystalline, single-phase and multi-phase microstructures have been produced [4]. This earlier review includes 408 unique alloys drawn from seven different major alloy families – 3d TM alloys and refractory CCAs (RCCAs) are the two most common families. Alloys were often characterized in the as-cast condition, and many alloys are also characterized after various thermo-mechanical treatments, giving 648 different microstructural reports. Twenty-three different crystalline phases were reported, producing a large number of microstructures. We focus the discussion on the unusual, unique or attractive microstructures rather than describing all the microstructures produced.

Microstructures in the 3d TM family are dominated by the austenitic, fcc phase when Al is absent from the alloy composition. Essentially every alloy in this category contains at least 1 fcc phase, a notable exception is $CoFeMnTi_xV_yZr_z$ ($0.5 \leq x \leq 2.5$, $0.4 \leq y \leq 3$, $0.4 \leq z \leq 3$), which forms a single-phase Laves (C14) microstructure [24]. The bcc, σ, C14 and $L1_2$ phases are often found with the fcc phase in 3d TM alloys. 3d TM alloys that include Al usually contain the austenitic fcc phase when the Al content is low, contain fcc+bcc phases for intermediate Al levels, and have microstructures dominated by bcc and ordered bcc phases for high Al levels [4,6,10] (Fig. 2a). The specific levels of Al where these transitions occur depend on the number and types of 3d transition metal principal elements. Several alloys contain both fcc and ordered fcc ($L1_2$) phases, similar to superalloys. However, beyond changing the grain size of the principal phase, very few efforts have been undertaken in 3d TM alloys to control major microstructural features such as size, volume fraction and distribution of second phases.

A recent review of RCCAs shows that microstructures are dominated by the disordered bcc phase [12]. The most common additional phases are Laves, B2, M_5Si_3 and Al_xZr_5. As with 3d TM alloys, systematic studies to control microstructural features and hence mechanical properties have not been a major focus. However, several RCCAs have a significant volume fraction of nanometer-sized, atomically coherent, cuboidal bcc particles uniformly distributed in a B2 matrix. These alloys belong to the $Al_vMo_wNbTa_xTi_yZr_z$ family, where ($0.25 \leq v \leq 1$, $0 \leq w \leq 0.5$, $0.5 \leq x \leq 1$, $1 \leq y \leq 1.5$, $1 \leq z \leq 1.3$). One such alloy also has $V_{0.2}$. These microstructures are a bcc-based analog to those that have been carefully engineered between the disordered, fcc γ phase and the ordered, $L1_2$ γ' phase in nickel-based superalloys. As a result, these alloys are called refractory HEA superalloys [25]. These RCCA microstructures are 'inverted' from conventional γ/γ' microstructures, since the stronger but less ductile B2 phase is continuous, whereas the disordered γ phase is continuous in superalloy microstructures (Fig. 2b). As a result, these RCCAs have exceptional strength but have inadequate compressive ductility at

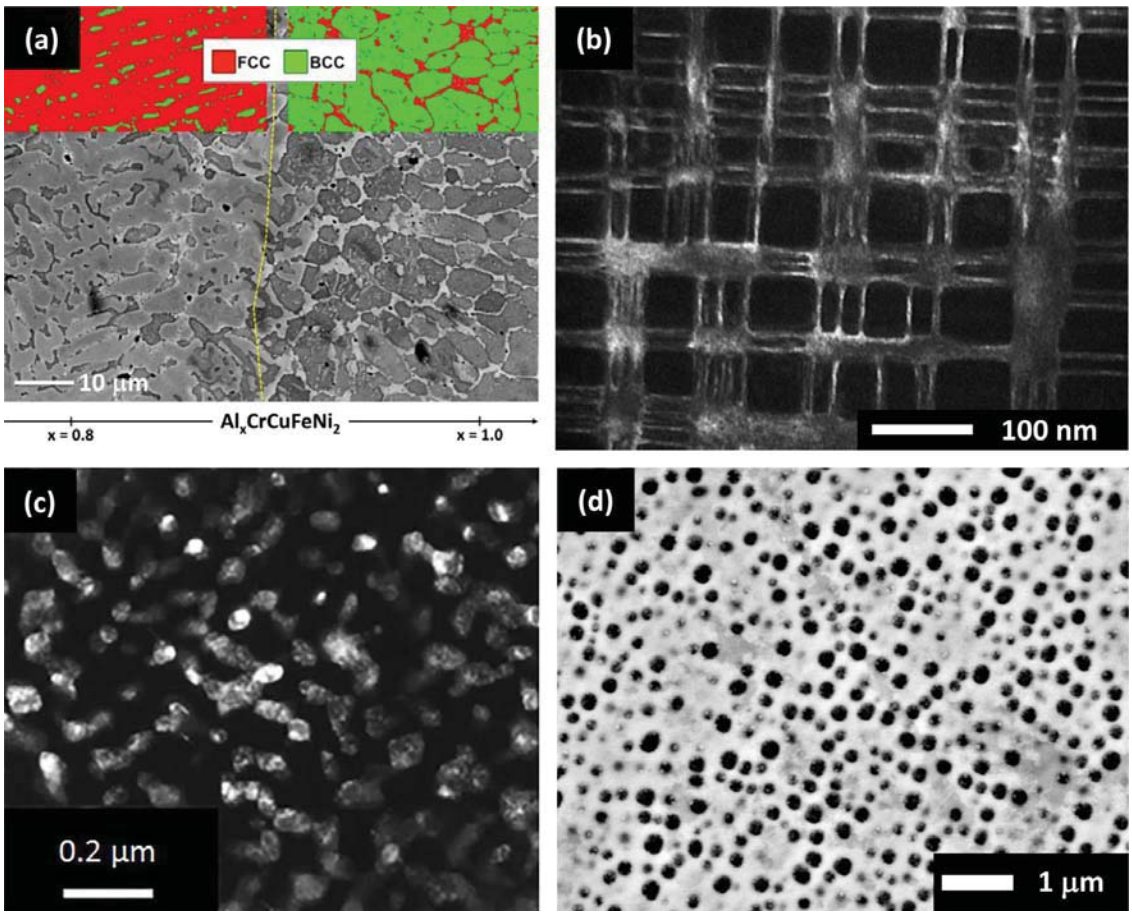

Fig. 2. Microstructures of CCAs. (a) Backscattered Scanning Electron Microscope (SEM) image showing microstructural transition from $x = 0.8$ to $x = 1.0$ along compositionally graded LENS-deposited $Al_xCrCuFeNi_2$; electron backscatter diffraction (EBSD) phase maps showing fcc (red) and bcc (green) distribution [27]. (b) Dark-field transmission electron microscope (TEM) micrograph of the nano-phase structure of $AlMo_{0.5}NbTa_{0.5}TiZr$ with bcc precipitates (bright contrast) in B2 matrix (dark contrast) ([28], reprinted by permission of Taylor & Francis Ltd.). (c) Dark-field image with B2 precipitates (bright contrast) in disordered bcc matrix (dark contrast) for the $Al_{0.5}NbTa_{0.8}Ti_{1.5}V_{0.2}Zr$ homogenized at 1200°C for 24 h, solutionized at 1400°C for 20 min and annealed for 120 h at 600°C (from [26]). (d) SEM micrograph of spherical $Ni_3(Ti,Al)$ precipitates in a fcc disordered matrix for the $(CoCrFe)_{50}Ni_{40}(TiAl)_{10}$ composition [29].

room temperature. This microstructure has been reversed through thermal treatments, producing discrete B2 particles in a continuous, disordered bcc matrix (Fig. 2c) [26]. This microstructural change improves the room temperature compressive ductility, while maintaining high yield strengths at both room and elevated temperature.

Relatively limited numbers of CCAs have been produced in other families. The CCA brasses and bronzes use the equimolar CuMnNi base with additions of Al, Sn and/or Zn [18]. These microstructures are dominated by the disordered fcc (A1) phase, and the volume fractions of ordered B1, B2 and Heusler ($L2_1$) phases increase with increasing Al, Sn and Zn concentrations. Recently reported light metal CCAs all have AlLiMg, and also contain Cu, Sc, Sn or Zn [4]. These alloys usually have an fcc phase, and can also contain hcp, A5, DO_2 or C16 phases. Two 4f transitional metal alloys use hcp elements, and the CCA microstructures are predominantly hcp [15].

3.2. Unusual properties

3.2.1. Thermodynamic, kinetic, physical and functional properties

Many unique or unusual properties have been proposed for CCAs. Four 'core effects' are defined in early papers, including high configurational entropy, large lattice distortions due to the high concentrations of multiple principal elements with different atomic volumes, and sluggish diffusion. The configurational entropy of actual CCAs is very difficult to measure, but the frequent occurrence of multiple phases and computational results indicating short-range atomic ordering [30] both suggest that the configurational entropy of solid solutions in many CCAs is less than ideal values. However, measured chemistries often show that there are more principle elements in CCA ordered phases than there are sublattices [26,30]. This requires elemental mixing on at least one of the sublattices, increasing configurational entropies relative to ordered, intermetallic phases where each sublattice is dominated by a single element. Early papers proposed that diffusion might be unusually sluggish in HEAs. The first measurement of diffusion in an HEA showed that diffusion was actually slightly faster than in compositionally simpler alloys when comparison was made at identical temperatures [31]. Even when comparing at

similar homologous temperatures, it has been shown that HEA diffusion is within the range of metallic elements and compositionally simpler alloys with the same crystal structure [21,32]. Nevertheless, diffusion in CCAs can be complex, and both positive and negative cross-terms have been observed. Approaches to measure lattice distortion in CCAs are still evolving [33,34]. Early results show that HEA lattice distortions are significant, of the order of 1%, but they are not anomalously large relative to concentrated binary or ternary alloys.

A recent review evaluates the data available for functional properties of CCAs [22]. Overall, functional CCAs do not seem to offer unusual or exceptional magnetic, magneto-caloric, electrical resistivity, thermal conductivity, thermo-electric, superconducting or hydrogen storage properties. However, efforts to intentionally design CCAs for these functional properties have hardly begun, and in many cases the functional properties have been measured on alloys intended for other purposes. As a result, additional work in this field is still recommended. There are three functional properties, however, where CCAs appear to offer attractive properties. In general, CCAs seem to possess good corrosion resistance, and have corrosion and pitting potentials that are in the range of those of austenitic and ferritic stainless steels [35]. As with conventional stainless steels, the elements Ti, Cr, and Mo seem to improve the corrosion performance of CCAs. The resistance of CCAs to irradiation-induced swelling damage appears to be significantly better than currently used alloys under similar exposures [36], suggesting an important area for additional work. Magnetic properties of HEAs and CCAs are compared with commercial soft and hard magnets in Fig. 3a where the saturation magnetization is plotted against the coercivity. In contrast with currently best magnets such as Nd–Fe–B and SmCo, the coercivity of CCAs derive from phase separation (spinodal decomposition) into periodic, nanoscaled, two-phase microstructures of interconnected hard and soft phases [5], offering the opportunity to design high performance magnets to meet the demand for rare earth-free magnetic materials with high energy product and high mechanical strength. Finally, the ability to depart from alloy bases dominated by a single element offers the new possibility to tailor physical properties such as density and stiffness. This allows alloys to be intentionally designed across the full spectrum of specific properties such as specific strength and specific stiffness, and current CCAs are already filling gaps between conventional alloy systems (Fig. 3b) [10].

3.2.2. Mechanical properties and associated deformation mechanism

By far the largest amount of work has been performed on the deformation and mechanical properties of CCAs. The understanding of strengthening and deformation mechanisms is critical for the development of such materials, especially for future structural applications. These mechanisms have been extensively studied in fcc structure of 3d TM alloys [42–44], but in-depth studies in bcc HEAs are scarce, probably due to the low ductility of many RCCAs, especially at room temperature (RT). The only available reports in the literature for deformation of bcc alloys are for RCCAs that are ductile at RT [12]. The plasticity of 3d TM alloys and RCCAs is typically provided by conventional mechanisms, so that deformation mechanisms have been mainly associated with dislocation glide and/or twinning processes, according to the HEA structure (fcc or bcc).

Among CCAs with fcc structures, the single-phase CoCrNi-based family is the most widely described. Substantial efforts have been made to understand the unusual increase of both strength and ductility with decreasing temperature [45–48]. Deformation mainly occurs by the planar glide of $a/2 < 110 >$ dislocations on {111} planes in the first stages of plasticity over a broad range of temperature (77–873 K) [49]. The presence of stacking fault ribbons shows the dissociated character of dislocations and highlights the key role of stacking fault energy (SFE) in the deformation process. In fcc single-phase CCAs, the SFE critically depends on composition and has values from 18–38 mJ/m^2 in the Co–Cr–Fe–Mn–Ni system [50]: ∼20 mJ/m^2 is obtained in the ternary CoCrNi system [50,51] and ∼30 mJ/m^2 for the CoCrFeMnNi single phase HEA [50, 52,53]. The chemical complexity of HEAs can give local chemical variations much larger than those in more dilute alloys, producing local variations in SFE that challenge the standard concept of a fixed SFE in a given alloy. Careful studies of the separation between leading and trailing partial dislocations in CoCrFeMnNi show a large variability in dissociation distances, supporting this idea [54]. The SFE of CoCrFeMnNi is also strongly affected by temperature, and *ab initio* calculations show a decrease from 21 to 3.4 mJ/m^2 between RT and 0 K [53]. The reduction appears to be connected to the evolution of chemical and magnetic contributions with temperature. First principles calculations also highlight the existence of negative SFEs in some ternary and quaternary single-phase alloys at 0 K [45,55]. Such results indicate a possible fcc to hcp phase transition at low temperatures by the spontaneous emission of partial dislocations from the parent fcc phase. This could explain the abundant twinning activity at low temperature in CoCrNi and CoCrFeMnNi.

Low SFEs have significant consequences for deformation mechanisms in fcc HEAs – they lead to large dislocation dissociations which support the planar character of dislocation glide by inhibiting cross-slip at low strains [52] but also lead to the activation of twinning which becomes an important deformation mode in HEAs with low SFEs [49,56]. Twinning activity is all the more intense that deformation is increased but twin volume fractions remain relatively low and do not exceed 5% [56]. The critical resolved shear stress is temperature independent, reaching 260 ± 30 MPa and 235 ± 10 MPa between 77 K and 298 K for polycrystalline CoCrNi and CoCrFeMnNi, respectively. Such values correlate well with experiments on [001] single crystals for which 210 ± 10 MPa is obtained at liquid nitrogen temperature [57]. Twinning mechanisms are still under consideration but involve the motion of $a/6 < 112 >$ Shockley partials and the possible cross-slip of dislocations with $a/2 < 110 >$ Burgers vector from primary to conjugate planes [58].

The presence of nanotwins creates new interfaces which decrease the free mean path of dislocations and produces a dynamic Hall-Petch effect. The activation of several twinning systems is likely to promote a 3D twin architecture insuring a dual increase of both strength and ductility: interfaces appear as strong barriers for dislocation motion but offer new

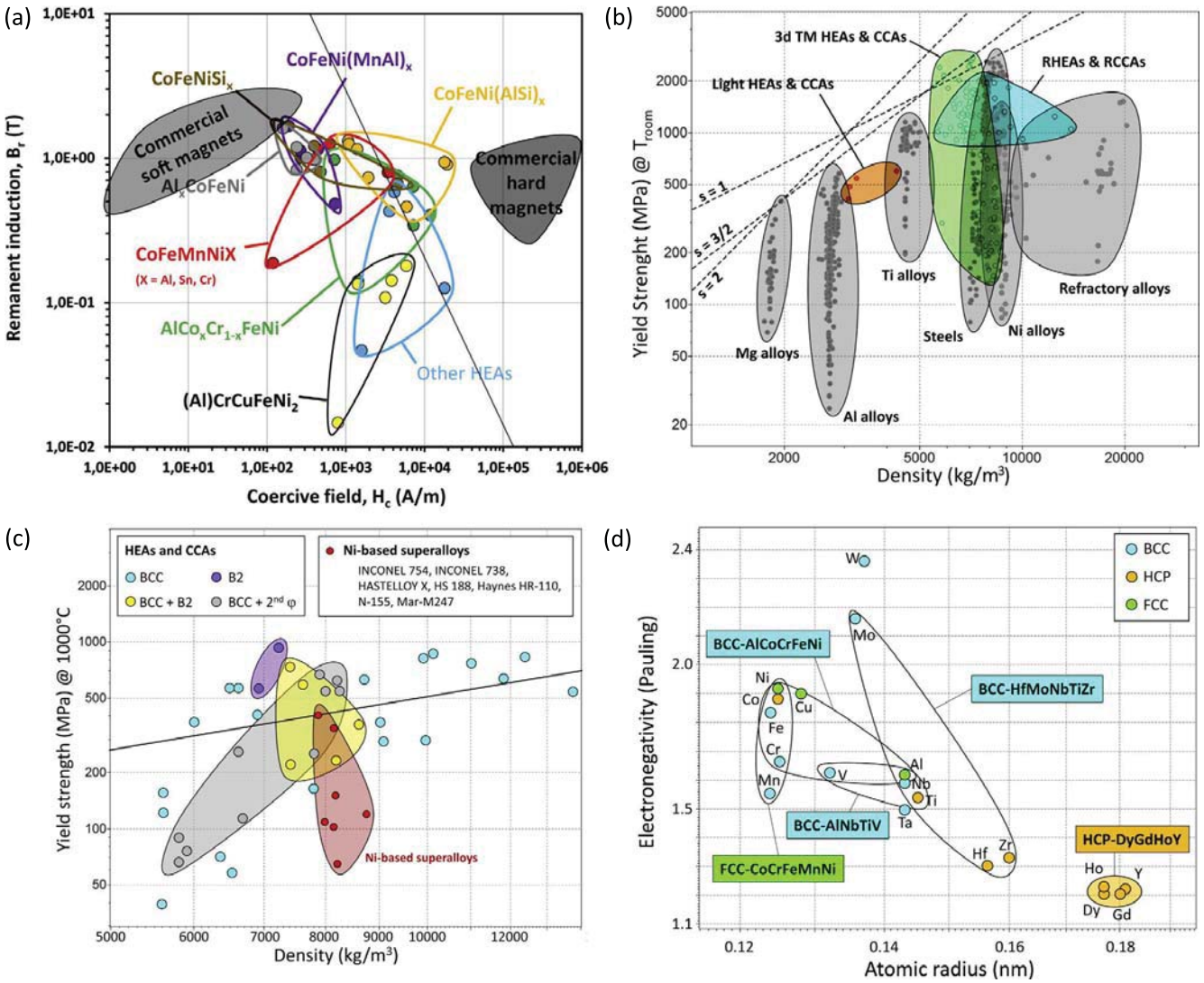

Fig. 3. Materials property spaces for HEAs and CCAs. (a) Remnant induction vs. coercivity for conventional magnets and magnetic HEAs and CCAs (data taken from [5,37–40]). Individual alloys (shown as circles) are enclosed in large bubbles that represent alloy classes (one class is a unique combination of principal elements). The line gives the energy product. HEAs and CCAs lie between soft magnetic materials (on the left of the chart) and hard magnetic materials (on the right). (b) Room-temperature yield strength vs. density of conventional metal alloys, HEAs and CCAs ([10], reprinted by permission of Elsevier). Individual alloys (shown as open and closed circles) are enclosed in large bubbles that represent alloy families. This chart displays data for about 1220 commercial and 120 HEAs and CCAs. The dashed lines give performance indices for uniaxial loading (slope, $s = 1$), beam bending ($s = 3/2$) and panel bending ($s = 2$). Materials above a performance index line have higher values of that performance index than those below it, so that lighter and stronger structures can be made from alloys above the line. 3d transition metal and refractory metal HEAs and CCAs overlap with steels and Ni alloys and begin to fill the gap between steels and Ti alloys, offering new materials design options. Light metal CCAs span the gap between conventional Al and Ti alloys. (c) Yield strength vs. density at 1000°C for refractory metal HEAs and CCAs (RHEAs and RCCAs) and commercial Ni-based superalloys (data from [10,41]). RHEAs and RCCAs have been colored to identify crystal structure. The line gives performance index for uniaxial loading (slope, $s = 1$, corresponding to the material index σ^Y/ρ where σ^Y and ρ are the yield strength and the density, respectively). The performance index line is placed on the highest value of specific yield strength for Ni alloys, so RHEAs (bcc) and RCCAs (e.g., bcc + B2) above this performance index line outperform the best Ni alloys at 1000°C. This chart shows the potential of RHEAs and RCCAs for high temperature application where high strength-to-density ratios (i.e. high specific strength) are required. (d) Electronegativity against atomic radius. The elements have been colored to identify crystal structure. Experiments suggest that the Hume–Rothery rules – according to which substitutional solid solutions are observed mostly in alloys of elements with similar atomic radius, crystal structure and electronegativity – are relaxed somewhat in multi-component systems. For instance, a CoCrFeNiMn alloy forms a single fcc solid solution even though the components have three different structures. This chart was inspired by a figure shared by Mike Ashby. It was made with the Cambridge Education Software (CES) Edupack from Granta Design.

pathways for $a/6 < 112 >$ dislocations. At the macroscopic scale this latter effect causes a pronounced increase of work-hardening and also increases the ductility by postponing the achievement of Considere's criterion.

Unlike fcc HEAs, little is known about strengthening and deformation mechanisms in bcc HEAs. Reports are limited to ductile HEAs containing Hf, Nb, Ti, Zr, and/or Ta [59–63]. Deformation processes are carried out by dislocation plasticity and results show the key role of $a/2 < 111 >$ screw dislocations in the mechanical behavior of bcc HEA solid solutions [64]. In HfNbTaTiZr, deformation rapidly becomes heterogeneous and distinct, alternating bands of dense deformation activity

and dislocation free zones appear [64,65]. Screw dislocations appear of limited mobility, suggesting complex, extended dislocation cores as are typically observed in dilute bcc metals and alloys at low temperatures. This is also consistent with the evidence of dislocation glide on {112} planes. Short-range obstacles control the plastic behavior and hardening is mainly related to the evolution of internal stresses during deformation processes in some solid solutions [65]. Activation volumes measured using relaxation tests reveal values from 5–94 b^3 (with $b = a/2 < 111 >$) between cryogenic temperatures and 200°C, compatible with a lattice friction dominated mechanism (Peierls barriers), in the first approximation [64–67]. In the classical thermally activated deformation formalism, activation energies for kink pair nucleation on screw defects between 0.69 and 0.84 eV have been obtained [67]. However, extensive debris in the wake of screw dislocations suggest strong interactions of such defects with possible local composition fluctuations of the solid solution. Consequently, strengthening may be associated with formation of superjogs which represent strong athermal barriers for moving dislocations [68].

3.2.3. Strengthening mechanisms

Due to the intrinsic nature of CCAs, solid solution strengthening is considered to have a crucial impact on the mechanical properties of such materials. So far, reported hardening models for CCAs have considered mismatch terms from the significant local mismatch in both elastic properties and atomic volumes of constituent atoms [59,70,71] but consensus has not yet been reached and more work is needed: conventional strengthening models alone could not explained the measured mechanical properties. In the same way, there has been essentially no work applying standard particulate hardening models to CCAs.

The strengthening in CCAs can result from the specific deformation mechanisms described above and may also rely on unusual features. Hardening from transformation-induced plasticity (TRIP) and twinning-induced plasticity (TWIP) is often observed, since CCAs offer new opportunities for tailoring stacking fault energies (SFEs) and phase stabilities that control these mechanisms. Significant local variations in SFE is seen from direct experimental measurements, which show a significant difference in the separations between leading and trailing partial dislocations [54]. The implications of this new feature on hardening and deformation have not yet been established. HEAs show a typical Hall-Petch relationship between grain size and yield strength [49], however, CCAs show an unusual strengthening effect due to frustration of magnetic moments [69]. Specifically, the equimolar CoCrNi alloy is stronger than the elemental constituents, and some of this strengthening results from a magnetic frustration term. However, a continued increase in compositional complexity, from CoCrNi to CoCrFeMnNi, decreases the strength due to a reduction in the magnetic frustration of the equimolar quinary alloy.

4. Accelerated alloy development – closing the complexity gap

4.1. Alloy development

The improvement of the mechanical properties of promising HEAs requires different alloying strategies which derive from traditional metallurgy. The approaches rely on the introduction of strong barriers to dislocation motion. These design procedures for the development of new alloys also depend crucially on the operating temperature of the target application. There are three ways to harden HEAs, all of them are built on the addition of appropriate elements to produce targeted microstructures. Each strategy aims to: (i) promote the formation of multi-phase HEAs, (ii) obtain a controlled nano-precipitation in a compositionally complex solid solution for high temperature applications, and (iii) control alloy chemistry to activate induced plasticity effects under stress, mainly at room temperature. Strategies (ii) and (iii) will be discussed in the following paragraphs as they correspond to the main trends.

Substantial increases in strength – while keeping reasonable ductility – could be achieved if precipitation is controlled, *i.e.* if the precipitates are coherent and finely dispersed in the matrix. A targeted strategy for HEAs is very similar to that developed in duplex γ–γ' superalloys and leads to the research of hardened fcc- or bcc-HEAs with nanosized reinforcing phases [25,72]. In this respect, minor additions of titanium and aluminum in Co–Cr–Fe–Ni-based systems have led to interesting results with the formation of Ni_3(Ti,Al)-type precipitates with the $L1_2$ structure in a disordered fcc matrix (Fig. 2d) [72,73]. A homogeneous distribution of nanometer-sized, ordered $L1_2$ (γ') precipitates within the fcc matrix has been obtained in $Al_{0.3}$CoCrFeNi after controlled thermo-mechanical treatments [74]. Such precipitation is predicted by thermodynamic calculations over a broad composition range, but the actual two-phase fcc + $L1_2$ domain is rather limited due to chemical complexity of the alloying system and the appearance of multiple intermetallic phases (Fig. 4). However, successful exploration has been carried out in Al–Co–Cr–(Fe)–Ni–Ti alloys [72,73,75] and in complex Co–Cr–Cu–Fe–Ni compositions [76]. Coherent nano-scaled precipitates are found in $(CoCrFeNi)_{94}Ti_2Al_4$ with different morphologies, and the small precipitate sizes (10–100 nm) induce a considerable increase of yield strength at room temperature: over 1 GPa is obtained, which is 5 times higher than the strength of the CoCrFeNi equimolar alloy [72]. Precipitation hardening contributes significantly to the yield strength and is even considered as the dominant strengthening mechanism at room temperature in alloys containing nano-scale $L1_2$ Ni_3(Ti,Al) and Ni_2AlTi precipitates [72]. Precipitation-hardened HEAs exhibit improved tensile properties at high temperature thanks to the good thermal stability of the $L1_2$ phase [77]: enhanced properties are observed for $Al_{10}Co_{25}Cr_8Fe_{15}Ni_{36}Ti_6$ in the 400–800°C range [75] and for $(CoCrFeNi)_{94}Ti_2Al_4$ between 750°C and 900°C [78]. In the latter case, particle shearing appears as the main active strengthening mechanism.

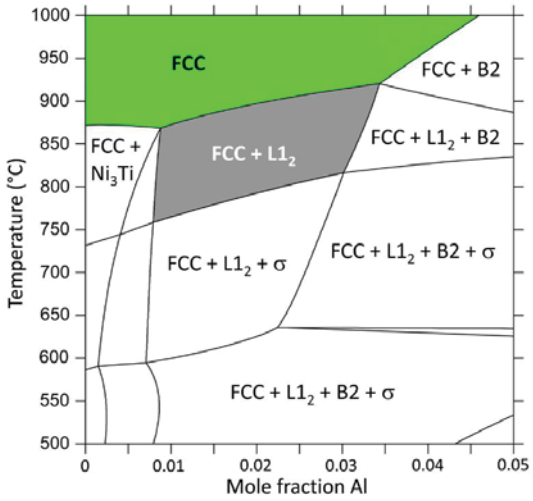

Fig. 4. Isopleth $(CoCrFeNi)_{0.98-x}Ti_{0.02}Al_x$ with x the atomic fraction of aluminum (TCHEA3 database, Thermocalc).

Precipitation hardening strategies appear more challenging in bcc HEAs and CCAs. The reasons are twofold: first, and contrary to fcc systems based on Ni, Co or Fe, CALPHAD modeling is uncertain as databases seem insufficiently reliable. Especially, the B2 phase is sometimes observed in RCCAs with Al, but thermodynamic models of the B2 phase are generally not included in CALPHAD databases. Second, there are very few observations of fine and thermally stable second-phase particles in bcc HEAs/CCAs. Several systems are likely to be strengthened by secondary phases but different proposed strategies often lead to brittle alloys due the precipitation of uncontrolled phases [79,80]. However recent efforts have yielded promising results in Al_2M_{14} (M=Co,Cr,Fe,Ni) [81] and in the Mo–Nb–Ta–Ti–Zr system with the addition of aluminum [82], where nano-precipitation of a coherent Nb,Ta,Mo-rich phase in an ordered B2 matrix (inverted duplex γ–γ' microstructure) is of particular interest [82]. The B2+bcc microstructure leads to impressive mechanical compressive properties up to 1000°C. The research is still in progress to optimize the microstructure design but very recent results on $Al_{0.5}NbTa_{0.8}Ti_{1.5}V_{0.2}Zr$ clearly show the potential of such systems [26]. After appropriate heat treatments, coherent and finely dispersed B2 precipitates are observed in the disordered bcc matrix (Fig. 2c). Mechanical properties are particularly attractive and provide a promising combination of high yield stress and good ductility [26].

Based on the approach initially developed for steels, TRansformation Induced Plasticity (TRIP) and/or Twinning Induced Plasticity (TWIP) effects have been successfully applied to HEAs. The first evidence of the TWIP effect in CCAs was shown in the quaternary $Co_{10}Cr_{10}Fe_{40}Mn_{40}$ fcc composition at room temperature [83]. The SFE was intentionally decreased by tuning the composition, and removing Ni from the quinary CoCrFeMnNi for this purpose. In $Co_{10}Cr_{10}Fe_{40}Mn_{40}$, twinning is activated at strains $>10\%$ and the work hardening evolution is very similar to that of TWIP steels. The design concept based on SFE has been pushed to its limits to induce an fcc-to-hcp phase transformation during mechanical testing to obtain highly hardenable dual-phase HEAs [84]. The benefits of this strategy are twofold: it takes advantage of the large solid solution strengthening effect due to the compositional complexity of HEAs, and it decreases the dislocation mean-path with the creation of new interfaces. The metastability-engineering approach has also been used in Co–Cr–Fe–Mn HEAs and particularly in $Co_{10}Cr_{10}Fe_{80-x}Mn_x$ for which TWIP, TRIP and TRIP dual-phase alloys have been designed by adjusting the Mn content [84,85]. For the lower Mn content ($x = 30$), dual-phase HEA is obtained and initially (prior to deformation) consists of γ (fcc) and ε (hcp) phases. At room temperature the $Co_{10}Cr_{10}Fe_{50}Mn_{30}$ alloy exhibits good mechanical properties due to the initial dual-phase microstructure and also from the synergy between dislocation slip, formation of stacking faults and stress-induced transformation of γ to ε [85].

TRIP effects have also been recently achieved in bcc HEAs. Mainly proposed for Ti-based CCAs, the strategy aims to increase both the ductility and work-hardening rate of these materials. Two visions have been proposed in the literature [86,87] but both lead to the design of CCA compositions whose (bcc) matrix will be destabilized during the deformation processes at room temperature. In HEAs, the idea was first developed from a semi-empirical strategy using two electronic parameters: one parameter (Bo) represents the average covalent bond strength between Ti and the alloying elements and the second parameter (Md) corresponds to the average d-orbital energy level [88]. By choosing appropriate elements, activation of TRIP and/or TWIP effects or dislocation glide is made possible in compositionally complex Ti-based alloys (Fig. 5). TRIP effects have been evidenced in a Ti-rich CCA with the presence of a large fraction of twinned martensite α" after mechanical testing. The obtained tensile behavior highlights the benefit of the stress-induced martensite with a high normalized work-hardening rate of 0.103 without loss of ductility in comparison of the HfNbTaTiZr reference alloy [86]. Such a strategy appears promising, but the destabilization of the β (bcc) phase by the use of Bo–Md diagram is limited to Ti-based alloys and is only possible at room temperature.

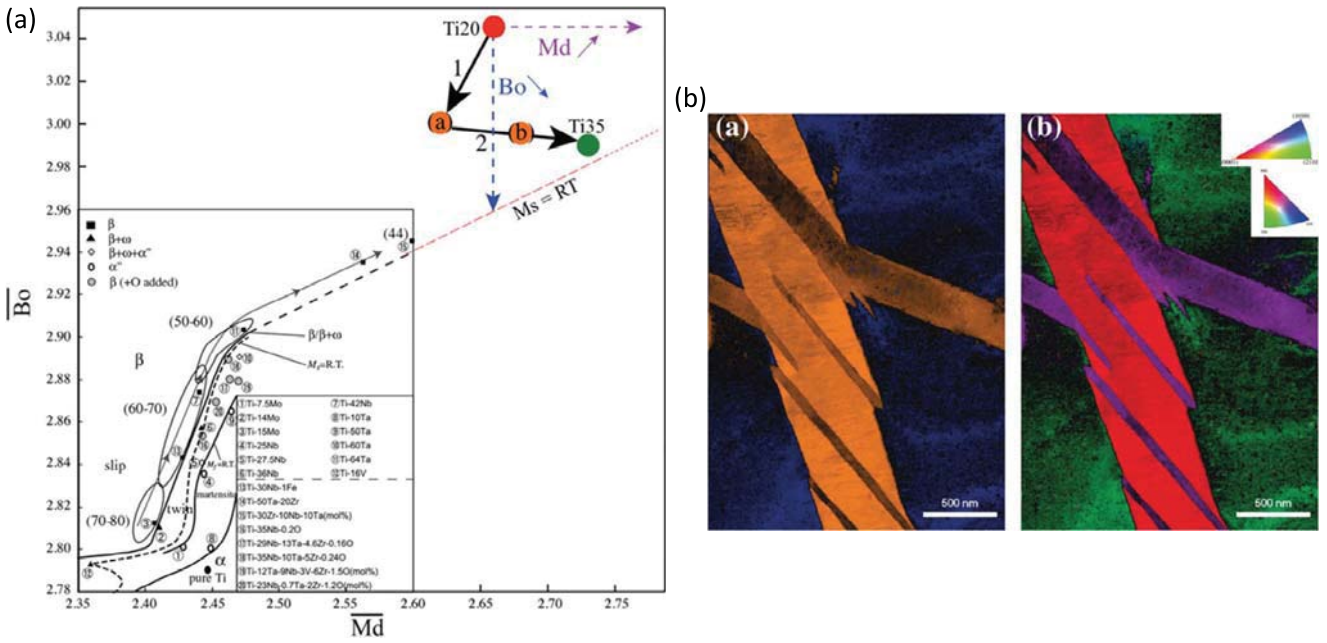

Fig. 5. (a) Bo-Md map used for conventional Ti-based alloys (bottom left) extrapolated to concentrated alloys (top right) [89]. The dashed line corresponds to the formation of martensite (Ms) from the bcc β phase. Starting from the equimolar HfNbTaTiZr composition, the coupled reduction of Ta and Nb contents and the increase of Hf, Nb and Ti ones lead to the definition of a non-equiatomic HfNbTaTiZr composition close to the martensite appearance zone; (b) Presence of stress induced α" (hcp) martensite in the initial β (bcc) phase after deformation. Phase mapping (left; bcc: blue; hexagonal: orange) and orientation mapping (right) (from [86]).

4.2. New tools and techniques

The HEA concept and its founding novel ideas encourage material scientists to change the way alloys are designed (see Section 2), offering the designer vast, new options for advanced materials. However, the HEA/CCA community must address several specific challenges and develop new knowledge to deliver novel alloys with better performance that will burst out of the lab to the marketplace. RCCAs are one of the most promising candidates for revolutionary improvements, since they represent the only major new idea that may satisfy the challenging needs for high temperature structural metals for use at 1200–1500°C. Fig. 3c illustrates the potential of RHEAs and RCCAs for high temperature application where high strength-to-density ratios (i.e. high specific strength) are required. RCCAs have both bcc (A2) and long-range ordered B2 phases, giving the opportunity to produce a bcc-based analog to γ–γ' nickel-based superalloy microstructures, which are characterized by a ductile, disordered fcc matrix and a high volume fraction of coherent, nanometer-sized long-range-ordered $L1_2$ precipitates. To reproduce this microstructural template in RCCAs, the extent of bcc and B2 phases and the bcc+B2 phase field boundaries have to be determined in both composition and temperature space. The B2 phase is often continuous in RCCAs, so the reaction pathways supporting controlled microstructural development through an adequate choice of composition and thermo-mechanical treatments need to be identified to produce the desired microstructure. The bcc phase is often ductile but can exhibit a brittle-to-ductile transition above room temperature, while the mechanical properties of B2 are strongly influenced by their degree of order, so that the fundamental mechanisms of deformation and fracture need to be studied and controlled in single-phase bcc (A2) and single-phase B2 materials to better understand constituent properties as a function of composition and temperature. Lattice compatibility is a key factor for obtaining high-temperature microstructure stability, so the lattice mismatch between the bcc matrix and the B2 particles needs to be finely tuned.

Experience gained from conventional alloy developments is likely to be an unreliable guide, and the potential for being surprised from basic intuition is significant with complex, baseless alloys (e.g., bcc phases are formed when adding a sufficient quantity of fcc-Al to fcc 3d TM HEAs, see also Fig. 3d). Additionally, the unprecedented high dimensionality of the HEA/CCA design space requires new approaches. To illustrate this vastness, the number of distinct alloy compositions contained in N-dimensional composition space (N is the number of alloying elements) at fixed temperature with compositional steps of δx (atom fraction) is given by:

$$\frac{(1/\delta x + 1)\,(1/\delta x + 2)\ldots(1/\delta x + (N-1))}{(N-1)!}$$

For example, this gives the large number of 96 million different compositions for the exploration of a senary system with a 1 at.% compositional step. Combined with the vast number of new alloy bases and the large number of processing parameters that affects properties at constant composition via the microstructure, the number of possible combinations to be explored becomes almost infinite. As a result, an exhaustive search for new HEAs/CCAs is an insurmountable task using

existing methods of exploration. Computations, modeling and data mining (e.g., machine learning), and combinatorial synthesis and processing on the experimental front, are expected to be very important to guide efforts to investigate this vast richness of complexity where there is little or no experience to guide intuition.

Predictive, computational thermodynamic (e.g., CALPHAD) allows high-order phase diagrams to be extrapolated from thermodynamic descriptions of lower-order systems (*i.e.* unaries → binaries, binaries → ternaries, nth-order → $(n+1)$th-order). This computer-aided design approach has been used to systematically explore the phase equilibria of over one hundred thousand equimolar alloy systems, enabling rapid identification of the most promising HEA candidates for structural applications [90,91]. A more general methodology for efficient screening and evaluation of non-equimolar alloys against a set of criteria uses both high-throughput computation and combinatorial experiments in a sequential manner [20, 92]. It is based on the principle that the time and resources spent evaluating each candidate alloy has an inverse relationship to the number of candidates – the larger is the number of candidates, the faster must be the initial evaluations. In the first stage of evaluation, high throughput phase diagram calculations use CALPHAD to select alloy compositions that can give the desired microstructures. Then, materials libraries with controlled composition gradients allow evaluation of properties that are relatively insensitive to microstructure. Finally, the candidates that have survived to this two-stage screening process are evaluated using materials libraries of fixed composition and controlled microstructure gradients. Diffusion couples [93], diffusion-multiples [94], laser additive manufacturing [6,27] and thin-film co-deposition [94] are the main methods which allow materials libraries to be fabricated with continuous composition and microstructure gradients.

The main limitation of the predictive capacity of the CALPHAD technique is due to the availability and reliability of the thermodynamic databases [7]. CALPHAD databases have been developed for traditional alloys, so the full thermodynamic assessment of the Gibbs energies is usually given only for compositions enriched with one main element. In contrast, HEAs and CCAs lie in the central regions of compositional space, far from the known boundaries delimited by the binary and ternary subsystems. Consequently, calculations in these vast composition spaces rely on the availability and quality of the descriptions of the lower order constituent systems and require large extrapolations from them. Reliability and accuracy of the predictions can thus become questionable when obtained from incomplete thermodynamic descriptions. Senkov et al. [90,91] defined a credibility criteria for CALPHAD calculations based on the fraction of fully thermodynamically assessed binary systems (FAB) and the fraction of fully assessed ternary systems (FAT) included in the database. Using these theoretical credibility criteria, Wertz et al. [95] recently demonstrated the importance of the number of assessed constituent binary systems and the compositional distance from them on the accuracy of ternary predictions. Their study compared equilibrium calculations for different level of credibility criteria (FAT = 0, FAB = 0, 1/3, 2/3) with baseline predictions that were assumed to be accurate because they were obtained from fully assessed ternaries (FAT = FAB = 1). There is a need to expand this approach to higher order systems to evaluate the ability to predict quaternary phase diagrams without ternary descriptions. This point is of prime interest because even specialized databases for HEAs, such as TCHEA3 from ThermoCalc which encompasses 26 elements, contains almost all the binary descriptions (295 over 325) but only 5% of the ternary are fully assessed (136 over 2600). None of the ternaries with refractory elements is fully-assessed in TCHEA3, so CALPHAD calculations rely entirely on the binary descriptions. Further, the CALPHAD technique cannot anticipate the formation of novel phases in a higher-order system that are not present in any of the bounding lower-order systems (principally from binary to ternary). This is a major drawback for the design of RHEAs because no B2 binary compounds with refractory elements are represented in CALPHAD databases. Consequently, current CALPHAD descriptions fail to predict the B2 phase in refractory alloys with three and more components, so thermodynamic databases must be improved.

The precursor work of Naka and Khan [96] in the 1990's explores complex aluminides, and is a mine of information for the RHEA designer. The authors show that complex B2 aluminides can be formed by mixing Al with two groups of metals, i.e. X = Ti, Zr, Hf, and Z = V, Nb, Ta, Cr, Mo, W, whereas there is no B2 in the subcomponent Al–X, Al–Z, and X–Z binaries. The existence of other complex refractory aluminide compounds has been reported in Ti–Al–Z systems, along the Ti_3Al–Z_3Al tie-line for compositions around Ti_2AlMo [97,98], Ti_2AlCr [99], Ti_2AlNb [100,101] and Ti_2AlTa [102–104], but the field of existence can be quite extended in the ternary compositional space around the X_2AlZ stoichiometry. In higher-order systems, only very few quaternary and quinary alloys were examined. The scarce results suggest that the B2 phase may extend over an even larger composition field and with different degrees of order depending on the composition and thermal treatments. Additional important sources of information for the existence of desired phases can be found in crystal structure stability databases, constructed either on empirical parameters (e.g., Villars's system of atomic parameters [105]), Mendeleev's number [106]) or quantum mechanics (e.g., Md and Bo electronic parameters [107] and ab-initio methods [108]). These sources can by interrogated through data mining to map and predict the stability of particular crystal structures in multicomponent systems or to find materials with desired properties [109,110]. Recently, the work of Menou et al. [111] provides an interesting example of the integration of different computational tools including data mining, predictive thermodynamic and multi-objective genetic algorithm, to more efficiently guide the design of fcc HEAs.

As materials science enters the era of materials informatics and big-data, the HEA/CCA community has the great opportunity to construct a dedicated database and share it in on-line repositories (examples include the AFLOWLIB.org consortium [112], the Materials Project [113], the Computational Materials Repository [114], The Electronic Structure Project [115], the Open Quantum Materials Database [116], and the Carnegie Mellon Alloy Database [117]).

CALPHAD, high-throughput experiments, high-throughput electronic structure and *ab initio* calculations, and new methods such as genetic algorithms and machine learning now offer new approaches to augment alloy discovery and development. These tools are already accelerating the development of conventional metal alloys. However, these same tools are

expected to play a more dominant role in the exploration, discovery and development of new alloys in the vast compositional and microstructural regions where intuition and experience are no longer adequate guides. In fact, the aggressive development, integration and application of these new tools and techniques are absolutely essential to discover and develop novel HEAs and CCAs with significant improvements over alloys produced conventionally using the historical approach of lightly-alloyed base elements.

5. Conclusion

Forged by design concepts that break with traditional metallurgy approaches, high-entropy alloys (HEAs) and complex concentrated alloys (CCAs) represent a new class of materials having the potential to provide attractive combinations of properties not achievable by other classes of metallic alloys. From the two pioneering approaches underlying the design of HEAs (i.e. increase of configurational entropy and exploration of central regions of phase diagrams for multi-principal elements systems), the metal alloy community has created many new metallic alloy families and inspired the development of new classes of ceramics, allowing the materials universe to be expanded towards a broader range of functional and structural properties, including corrosion resistance, resistance to irradiation damage, combination of high strength and ductility and high temperature mechanical behavior.

While the first generation of HEAs is dominated by single phase fcc and bcc alloys incorporating, respectively, 3d transition metals and refractory metals as principle elements, the next generation explores a broader landscape comprising multi-phase microstructures. Among the explored design strategies, the tuning of alloy chemistry to activate induced plasticity effects under stress or to promote the formation of secondary strengthening phases (e.g., fcc-based materials with the formation of hardenable $L1_2$ phase) have demonstrated interesting results. In particular, bcc + B2 two-phase microstructure, with discrete B2 precipitates dispersed within a continuous bcc matrix, open the way to the development of refractory metal CCAs with performance that may fill major needs for high temperature structural applications in the 1200–1500°C range.

The field inspires new challenges (e.g., efficient exploration of hyper-dimensional design space) that motivates the materials science community to pave the way for materials science data by integrating data-mining with computational and experimental approaches for materials discovery and innovation. We see great opportunity for the growing HEA/CCA community to create a common cloud platform that compiles and organizes their findings in shared repositories, allowing materials researchers to accelerate exploration and discovery at rates that may match the explosion of new alloys offered by HEAs.

References

[1] J.R. Davis, Metals Handbook, DESK EDITION, 2nd edition I, ASM International, Materials Park, Ohio, USA, 2003.
[2] B. Cantor, I.T.H. Chang, P. Knight, A.J.B. Vincent, Microstructural development in equiatomic multicomponent alloys, Mater. Sci. Eng. A, Struct. Mater.: Prop. Microstruct. Process. 375 (2004) 213–218, https://doi.org/10.1016/j.msea.2003.10.257.
[3] J.W. Yeh, S.K. Chen, S.J. Lin, J.Y. Gan, T.S. Chin, T.T. Shun, C.H. Tsau, S.Y. Chang, Nanostructured high-entropy alloys with multiple principal elements: Novel alloy design concepts and outcomes, Adv. Eng. Mater. 6 (2004) 299–303, https://doi.org/10.1002/adem.200300567.
[4] D.B. Miracle, O.N. Senkov, A critical review of high-entropy alloys and related concepts, Acta Mater. 122 (2017) 448–511, https://doi.org/10.1016/j.actamat.2016.08.081.
[5] T. Borkar, B. Gwalani, D. Choudhuri, C.V. Mikler, C.J. Yannetta, X. Chen, R.V. Ramanujan, M.J. Styles, M.A. Gibson, R. Banerjee, A combinatorial assessment of $AlxCrCuFeNi_2$ ($0 < x < 1.5$) complex concentrated alloys: microstructure, microhardness, and magnetic properties, Acta Mater. 116 (2016) 63–76, https://doi.org/10.1016/j.actamat.2016.06.025.
[6] D. Choudhuri, B. Gwalani, S. Gorsse, C.V. Mikler, R.V. Ramanujan, M.A. Gibson, R. Banerjee, Change in the primary solidification phase from fcc to bcc-based B2 in high entropy or complex concentrated alloys, Scr. Mater. 127 (2017) 186–190, https://doi.org/10.1016/j.scriptamat.2016.09.023.
[7] S. Gorsse, F. Tancret, Current and emerging practices of CALPHAD toward the development of high-entropy alloys and complex concentrated alloys, J. Mater. Res. (2018) 1–25, https://doi.org/10.1557/jmr.2018.152.
[8] G. Bracq, M. Laurent-Brocq, L. Perrière, R. Pirès, J.-M. Joubert, I. Guillot, The fcc solid solution stability in the Co–Cr–Fe–Mn–Ni multi-component system, Acta Mater. 128 (2017) 327–336, https://doi.org/10.1016/j.actamat.2017.02.017.
[9] M. Laurent-Brocq, L. Perrière, R. Pirès, Y. Champion, From high-entropy alloys to diluted multi-component alloys: range of existence of a solid-solution, Mater. Des. 103 (2016) 84–89, https://doi.org/10.1016/j.matdes.2016.04.046.
[10] S. Gorsse, D.B. Miracle, O.N. Senkov, Mapping the world of complex concentrated alloys, Acta Mater. 135 (2017) 177–187, https://doi.org/10.1016/j.actamat.2017.06.027.
[11] O.N. Senkov, G.B. Wilks, D.B. Miracle, C.P. Chuang, P.K. Liaw, Refractory high-entropy alloys, Intermetallics 18 (2010) 1758–1765, https://doi.org/10.1016/j.intermet.2010.05.014.
[12] O.N. Senkov, D.B. Miracle, K.J. Chaput, J.-P. Couzinie, Development and exploration of refractory high-entropy alloys—a review, J. Mater. Res. (2018) 1–37, https://doi.org/10.1557/jmr.2018.153.
[13] M. Feuerbacher, M. Heidelmann, C. Thomas, Hexagonal High-entropy Alloys, Mater. Res. Lett. 3 (2015) 1–6, https://doi.org/10.1080/21663831.2014.951493.
[14] R. Soler, A. Evirgen, M. Yao, C. Kirchlechner, F. Stein, M. Feuerbacher, D. Raabe, G. Dehm, Microstructural and mechanical characterization of an equiatomic YGdTbDyHo high-entropy alloy with hexagonal close-packed structure, Acta Mater. 156 (2018) 86–96, https://doi.org/10.1016/j.actamat.2018.06.010.
[15] A. Takeuchi, K. Amiya, T. Wada, K. Yubuta, W. Zhang, High-entropy alloys with a hexagonal close-packed structure designed by equi-atomic alloy strategy and binary phase diagrams, JOM 66 (2014) 1984–1992, https://doi.org/10.1007/s11837-014-1085-x.
[16] V.H. Hammond, M.A. Atwater, K.A. Darling, H.Q. Nguyen, L.J. Kecskes, Equal-channel angular extrusion of a low-density high-entropy alloy produced by high-energy cryogenic mechanical alloying, JOM 66 (2014) 2021–2029, https://doi.org/10.1007/s11837-014-1113-x.
[17] K.M. Youssef, A.J. Zaddach, C. Niu, D.L. Irving, C.C. Koch, A novel low-density, high-hardness, high-entropy alloy with close-packed single-phase nanocrystalline structures, Mater. Res. Lett. 3 (2015) 95–99, https://doi.org/10.1080/21663831.2014.985855.

[18] K.J. Laws, C. Crosby, A. Sridhar, P. Conway, L.S. Koloadin, M. Zhao, S. Aron-Dine, L.C. Bassman, High entropy brasses and bronzes – microstructure, phase evolution and properties, J. Alloys Compd. 650 (2015) 949–961, https://doi.org/10.1016/j.jallcom.2015.07.285.
[19] L. Kaye, S. Aron-Dine, A. Lim, L. Bassman, K. Laws, W. McKenzie, C. Healy, Making jewellery or other personal adornments, Patent application WO2017132725A1, 2017; n.d.
[20] D.B. Miracle, J.D. Miller, O.N. Senkov, C. Woodward, M.D. Uchic, J. Tiley, Exploration and development of high-entropy alloys for structural applications, Entropy 16 (2014) 494–525, https://doi.org/10.3390/e16010494.
[21] D.B. Miracle, High-entropy alloys: a current evaluation of founding ideas and core effects and exploring "nonlinear alloys", JOM 69 (2017) 2130–2136, https://doi.org/10.1007/s11837-017-2527-z.
[22] M.C. Gao, D.B. Miracle, D. Maurice, X.H. Yan, Y. Zhang, J.A. Hawk, High-entropy functional materials, J. Mater. Res. (2018) 1–18, https://doi.org/10.1557/jmr.2018.323.
[23] D.B. Miracle, Critical assessment 14: high-entropy alloys and their development as structural materials, Mater. Sci. Technol. 31 (2015) 1142–1147, https://doi.org/10.1179/1743284714Y.0000000749.
[24] Y.-F. Kao, S.-K. Chen, J.-H. Sheu, J.-T. Lin, W.-E. Lin, J.-W. Yeh, S.-J. Lin, T.-H. Liou, C.-W. Wang, Hydrogen storage properties of multi-principal-component CoFeMnTi(x)V(y)Zr(z) alloys, Int. J. Hydrog. Energy 35 (2010) 9046–9059, https://doi.org/10.1016/j.ijhydene.2010.06.012.
[25] O.N. Senkov, D. Isheim, D.N. Seidman, A.L. Pilchak, Development of a refractory high entropy superalloy, Entropy 18 (2016), https://doi.org/10.3390/e18030102.
[26] V. Soni, O.N. Senkov, B. Gwalani, D.B. Miracle, R. Banerjee, Microstructural design for improving ductility of an initially brittle refractory high-entropy alloy, Sci. Rep. 8 (2018) 8816, https://doi.org/10.1038/s41598-018-27144-3.
[27] S. Gorsse, C. Hutchinson, M. Gouné, R. Banerjee, Additive manufacturing of metals: a brief review of the characteristic microstructures and properties of steels, Ti-6Al-4V and high-entropy alloys, Sci. Technol. Adv. Mater. 18 (2017) 584–610, https://doi.org/10.1080/14686996.2017.1361305.
[28] J.M. Sosa, J.K. Jensen, D.E. Huber, G.B. Viswanathan, M.A. Gibson, H.L. Fraser, Three-dimensional characterisation of the microstructure of an high-entropy alloy using STEM/HAADF tomography, Mater. Sci. Technol. 31 (2015) 1250–1258, https://doi.org/10.1179/1743284715Y.0000000049.
[29] T. Rieger, M. Laurent-Brocq, J.-P. Couzinie, 2018, personal communication.
[30] L.J. Santodonato, Y. Zhang, M. Feygenson, C.M. Parish, M.C. Gao, R.J.K. Weber, J.C. Neuefeind, Z. Tang, P.K. Liaw, Deviation from high-entropy configurations in the atomic distributions of a multi-principal-element alloy, Nat. Commun. 6 (2015) 5964, https://doi.org/10.1038/ncomms6964.
[31] K.-Y. Tsai, M.-H. Tsai, J.-W. Yeh, Sluggish diffusion in Co–Cr–Fe–Mn–Ni high-entropy alloys, Acta Mater. 61 (2013) 4887–4897, https://doi.org/10.1016/j.actamat.2013.04.058.
[32] M. Vaidya, K.G. Pradeep, B.S. Murty, G. Wilde, S.V. Divinski, Bulk tracer diffusion in CoCrFeNi and CoCrFeMnNi high-entropy alloys, Acta Mater. 146 (2018) 211–224, https://doi.org/10.1016/j.actamat.2017.12.052.
[33] L.R. Owen, E.J. Pickering, H.Y. Playford, H.J. Stone, M.G. Tucker, N.G. Jones, An assessment of the lattice strain in the CrMnFeCoNi high-entropy alloy, Acta Mater. 122 (2017) 11–18, https://doi.org/10.1016/j.actamat.2016.09.082.
[34] Y. Tong, G. Velisa, T. Yang, K. Jin, C. Lu, H. Bei, J.Y.P. Ko, D. Pagan, R. Huang, Y. Zhang, L. Wang, F.X. Zhang, Probing local lattice distortion in medium- and high-entropy alloys, arXiv:1707.07745, 2017.
[35] Y. Qiu, S. Thomas, M.A. Gibson, H.L. Fraser, N. Birbilis, Corrosion of high-entropy alloys, Mater. Degrad. 1 (2017) 15, https://doi.org/10.1038/s41529-017-0009-y.
[36] S. Xia, Z. Wang, T. Yang, Y. Zhang, Irradiation behavior in high-entropy alloys, J. Iron Steel Res. Int. 22 (2015) 879–884, https://doi.org/10.1016/S1006-706X(15)30084-4.
[37] T. Zuo, M.C. Gao, L. Ouyang, X. Yang, Y. Cheng, R. Feng, S. Chen, P.K. Liaw, J.A. Hawk, Y. Zhang, Tailoring magnetic behavior of CoFeMnNiX (X = Al, Cr, Ga, and Sn) high-entropy alloys by metal doping, Acta Mater. 130 (2017) 10–18, https://doi.org/10.1016/j.actamat.2017.03.013.
[38] P. Li, A. Wang, C.T. Liu, Composition dependence of structure, physical and mechanical properties of FeCoNi(MnAl)(x) high-entropy alloys, Intermetallics 87 (2017) 21–26, https://doi.org/10.1016/j.intermet.2017.04.007.
[39] P. Li, A. Wang, C.T. Liu, A ductile high-entropy alloy with attractive magnetic properties, J. Alloys Compd. 694 (2017) 55–60, https://doi.org/10.1016/j.jallcom.2016.09.186.
[40] L. Liu, J.B. Zhu, J.C. Li, Q. Jiang, Microstructure and magnetic properties of FeNiCuMnTiSn$_x$ high-entropy alloys, Adv. Eng. Mater. 14 (2012) 919–922, https://doi.org/10.1002/adem.201200104.
[41] O.N. Senkov, D.B. Miracle, K.J. Chaput, J.-P. Couzinie, Development and exploration of refractory high-entropy alloys – a review, J. Mater. Res. 33 (2018) 1–37, https://doi.org/10.1557/jmr.2018.153.
[42] G. Laplanche, A. Kostka, O.M. Horst, G. Eggeler, E.P. George, Microstructure evolution and critical stress for twinning in the CrMnFeCoNi high-entropy alloy, Acta Mater. 118 (2016) 152–163, https://doi.org/10.1016/j.actamat.2016.07.038.
[43] Z. Zhang, M.M. Mao, J. Wang, B. Gludovatz, Z. Zhang, S.X. Mao, E.P. George, Q. Yu, R.O. Ritchie, Nanoscale origins of the damage tolerance of the high-entropy alloy CrMnFeCoNi, Nat. Commun. 6 (2015) 10143, https://doi.org/10.1038/ncomms10143.
[44] F. Otto, A. Dlouhy, C. Somsen, H. Bei, G. Eggeler, E.P. George, The influences of temperature and microstructure on the tensile properties of a CoCrFeMnNi high-entropy alloy, Acta Mater. 61 (2013) 5743–5755, https://doi.org/10.1016/j.actamat.2013.06.018.
[45] Z. Zhang, H. Sheng, Z. Wang, B. Gludovatz, Z. Zhang, E.P. George, Q. Yu, S.X. Mao, R.O. Ritchie, Dislocation mechanisms and 3D twin architectures generate exceptional strength-ductility-toughness combination in CrCoNi medium-entropy alloy, Nat. Commun. 8 (2017) 14390, https://doi.org/10.1038/ncomms14390.
[46] Z. Zhang, M.M. Mao, J. Wang, B. Gludovatz, Z. Zhang, S.X. Mao, E.P. George, Q. Yu, R.O. Ritchie, Nanoscale origins of the damage tolerance of the high-entropy alloy CrMnFeCoNi, Nat. Commun. 6 (2015) 10143, https://doi.org/10.1038/ncomms10143.
[47] B. Gludovatz, A. Hohenwarter, D. Catoor, E.H. Chang, E.P. George, R.O. Ritchie, A fracture-resistant high-entropy alloy for cryogenic applications, Science 345 (2014) 1153–1158, https://doi.org/10.1126/science.1254581.
[48] B. Gludovatz, A. Hohenwarter, K.V.S. Thurston, H. Bei, Z. Wu, E.P. George, R.O. Ritchie, Exceptional damage-tolerance of a medium-entropy alloy CrCoNi at cryogenic temperatures, Nat. Commun. 7 (2016) 10602, https://doi.org/10.1038/ncomms10602.
[49] F. Otto, A. Dlouhy, C. Somsen, H. Bei, G. Eggeler, E.P. George, The influences of temperature and microstructure on the tensile properties of a CoCrFeMnNi high-entropy alloy, Acta Mater. 61 (2013) 5743–5755, https://doi.org/10.1016/j.actamat.2013.06.018.
[50] S.F. Liu, Y. Wu, H.T. Wang, J.Y. He, J.B. Liu, C.X. Chen, X.J. Liu, H. Wang, Z.P. Lu, Stacking fault energy of face-centered-cubic high-entropy alloys, Intermetallics 93 (2018) 269–273, https://doi.org/10.1016/j.intermet.2017.10.004.
[51] G. Laplanche, A. Kostka, C. Reinhart, J. Hunfeld, G. Eggeler, E.P. George, Reasons for the superior mechanical properties of medium-entropy CrCoNi compared to high-entropy CrMnFeCoNi, Acta Mater. 128 (2017) 292–303, https://doi.org/10.1016/j.actamat.2017.02.036.
[52] N.L. Okamoto, S. Fujimoto, Y. Kambara, M. Kawamura, Z.M.T. Chen, H. Matsunoshita, K. Tanaka, H. Inui, E.P. George, Size effect, critical resolved shear stress, stacking fault energy, and solid solution strengthening in the CrMnFeCoNi high-entropy alloy, Sci. Rep. 6 (2016) 35863, https://doi.org/10.1038/srep35863.
[53] S. Huang, W. Li, S. Lu, F. Tian, J. Shen, E. Holmström, L. Vitos, Temperature dependent stacking fault energy of FeCrCoNiMn high-entropy alloy, Scr. Mater. 108 (2015) 44–47, https://doi.org/10.1016/j.scriptamat.2015.05.041.
[54] T.M. Smith, M.S. Hooshmand, S.D. Esser, F. Otto, D.W. McComb, E.P. George, M. Ghazisaeidi, M.J. Mills, Atomic-scale characterization and modeling of 60 degrees dislocations in a high-entropy alloy, Acta Mater. 110 (2016) 352–363, https://doi.org/10.1016/j.actamat.2016.03.045.

[55] Y.H. Zhang, Y. Zhuang, A. Hu, J.J. Kai, C.T. Liu, The origin of negative stacking fault energies and nano-twin formation in face-centered cubic high-entropy alloys, Scr. Mater. 130 (2017) 96–99, https://doi.org/10.1016/j.scriptamat.2016.11.014.
[56] G. Laplanche, A. Kostka, O.M. Horst, G. Eggeler, E.P. George, Microstructure evolution and critical stress for twinning in the CrMnFeCoNi high-entropy alloy, Acta Mater. 118 (2016) 152–163, https://doi.org/10.1016/j.actamat.2016.07.038.
[57] I.V. Kireeva, Y.I. Chumlyakov, Z.V. Pobedennaya, A.V. Vyrodova, I. Karaman, Twinning in [001]-oriented single crystals of CoCrFeMnNi high-entropy alloy at tensile deformation, Mater. Sci. Eng. A, Struct. Mater.: Prop. Microstruct. Process. 713 (2018) 253–259, https://doi.org/10.1016/j.msea.2017.12.059.
[58] J. Liu, C. Chen, Y. Xu, S. Wu, G. Wang, H. Wang, Y. Fang, L. Meng, Deformation twinning behaviors of the low stacking fault energy high-entropy alloy: an in-situ TEM study, Scr. Mater. 137 (2017) 9–12, https://doi.org/10.1016/j.scriptamat.2017.05.001.
[59] O.N. Senkov, J.M. Scott, S.V. Senkova, D.B. Miracle, C.F. Woodward, Microstructure and room temperature properties of a high-entropy TaNbHfZrTi alloy, J. Alloys Compd. 509 (2011) 6043–6048, https://doi.org/10.1016/j.jallcom.2011.02.171.
[60] G. Dirras, J. Gubicza, A. Heczel, L. Lilensten, J.-P. Couzinie, L. Perriere, I. Guillot, A. Hocini, Microstructural investigation of plastically deformed $Ti_{20}Zr_{20}Hf_{20}Nb_{20}Ta_{20}$ high-entropy alloy by X-ray diffraction and transmission electron microscopy, Mater. Charact. 108 (2015) 1–7, https://doi.org/10.1016/j.matchar.2015.08.007.
[61] C.-C. Juan, M.-H. Tsai, C.-W. Tsai, W.-L. Hsu, C.-M. Lin, S.-K. Chen, S.-J. Lin, J.-W. Yeh, Simultaneously increasing the strength and ductility of a refractory high-entropy alloy via grain refining, Mater. Lett. 184 (2016) 200–203, https://doi.org/10.1016/j.matlet.2016.08.060.
[62] Y.D. Wu, Y.H. Cai, T. Wang, J.J. Si, J. Zhu, Y.D. Wang, X.D. Hui, A refractory $Hf_{25}Nb_{25}Ti_{25}Zr_{25}$ high-entropy alloy with excellent structural stability and tensile properties, Mater. Lett. 130 (2014) 277–280, https://doi.org/10.1016/j.matlet.2014.05.134.
[63] S. Sheikh, S. Shafeie, Q. Hu, J. Ahlstrom, C. Persson, J. Vesely, J. Zyka, U. Klement, S. Guo, Alloy design for intrinsically ductile refractory high-entropy alloys, J. Appl. Phys. 120 (2016) 164902, https://doi.org/10.1063/1.4966659.
[64] J.-P. Couzinie, L. Lilensten, Y. Champion, G. Dirras, L. Perriere, I. Guillot, On the room temperature deformation mechanisms of a TiZrHfNbTa refractory high-entropy alloy, Mater. Sci. Eng. A, Struct. Mater.: Prop. Microstruct. Process. 645 (2015) 255–263, https://doi.org/10.1016/j.msea.2015.08.024.
[65] L. Lilensten, J.-P. Couzinie, L. Perriere, A. Hocini, C. Keller, G. Dirras, I. Guillot, Study of a bcc multi-principal element alloy: tensile and simple shear properties and underlying deformation mechanisms, Acta Mater. 142 (2018) 131–141, https://doi.org/10.1016/jactamat.2017.09.062.
[66] M. Feuerbacher, M. Heidelmann, C. Thomas, Plastic deformation properties of Zr–Nb–Ti–Ta–Hf high-entropy alloys, Philos. Mag. 95 (2015) 1221–1232, https://doi.org/10.1080/14786435.2015.1028506.
[67] A.V. Podolskiy, E.D. Tabachnikova, V.V. Voloschuk, V.F. Gorban, N.A. Krapivka, S.A. Firstov, Mechanical properties and thermally activated plasticity of the $Ti_{30}Zr_{25}Hf_{15}Nb_{20}Ta_{10}$ high-entropy alloy at temperatures 4.2–350 K, Mater. Sci. Eng. A, Struct. Mater.: Prop. Microstruct. Process. 710 (2018) 136–141, https://doi.org/10.1016/j.msea.2017.10.073.
[68] S.I. Rao, C. Varvenne, C. Woodward, T.A. Parthasarathy, D. Miracle, O.N. Senkov, W.A. Curtin, Atomistic simulations of dislocations in a model bcc multicomponent concentrated solid solution alloy, Acta Mater. 125 (2017) 311–320, https://doi.org/10.1016/j.actamat.2016.12.011.
[69] C. Niu, C.R. LaRosa, J. Miao, M.J. Mills, M. Ghazisaeidi, Magnetically-driven phase transformation strengthening in high-entropy alloys, Nat. Commun. 9 (2018) 1363, https://doi.org/10.1038/s41467-018-03846-0.
[70] I. Toda-Caraballo, P.E.J. Rivera-Diaz-del-Castillo, Modelling solid solution hardening in high-entropy alloys, Acta Mater. 85 (2015) 14–23, https://doi.org/10.1016/j.actamat.2014.11.014.
[71] C. Varvenne, A. Luque, W.A. Curtin, Theory of strengthening in fcc high-entropy alloys, Acta Mater. 118 (2016) 164–176, https://doi.org/10.1016/j.actamat.2016.07.040.
[72] J.Y. He, H. Wang, H.L. Huang, X.D. Xu, M.W. Chen, Y. Wu, X.J. Liu, T.G. Nieh, K. An, Z.P. Lu, A precipitation-hardened high-entropy alloy with outstanding tensile properties, Acta Mater. 102 (2016) 187–196, https://doi.org/10.1016/j.actamat.2015.08.076.
[73] Y.L. Zhao, T. Yang, Y. Tong, J. Wang, J.H. Luan, Z.B. Jiao, D. Chen, Y. Yang, A. Hu, C.T. Liu, J.-J. Kai, Heterogeneous precipitation behavior and stacking-fault-mediated deformation in a CoCrNi-based medium-entropy alloy, Acta Mater. 138 (2017) 72–82, https://doi.org/10.1016/j.actamat.2017.07.029.
[74] B. Gwalani, S. Gorsse, D. Choudhuri, M. Styles, Y. Zheng, R.S. Mishra, R. Banerjee, Modifying transformation pathways in high-entropy alloys or complex concentrated alloys via thermo-mechanical processing, Acta Mater. 153 (2018) 169–185, https://doi.org/10.1016/j.actamat.2018.05.009.
[75] H.M. Daoud, A.M. Manzoni, N. Wanderka, U. Glatzel, High-temperature tensile strength of $Al_{10}Co_{25}Cr_8Fe_{15}Ni_{36}Ti_6$ compositionally complex alloy (high-entropy alloy), JOM 67 (2015) 2271–2277, https://doi.org/10.1007/s11837-015-1484-7.
[76] M.A. Manzoni, S. Singh, M.H. Daoud, R. Popp, R. Völkl, U. Glatzel, N. Wanderka, On the path to optimizing the Al–Co–Cr–Cu–Fe–Ni–Ti high-entropy alloy family for high temperature applications, Entropy 18 (2016), https://doi.org/10.3390/e18040104.
[77] Y.Y. Zhao, H.W. Chen, Z.P. Lu, T.G. Nieh, Thermal stability and coarsening of coherent particles in a precipitation-hardened $(NiCoFeCr)_{94}Ti_2Al_4$ high-entropy alloy, Acta Mater. 147 (2018) 184–194, https://doi.org/10.1016/j.actamat.2018.01.049.
[78] J.Y. He, H. Wang, Y. Wu, X.J. Liu, T.G. Nieh, Z.P. Lu, High-temperature plastic flow of a precipitation-hardened FeCoNiCr high-entropy alloy, Mater. Sci. Eng. A 686 (2017) 34–40, https://doi.org/10.1016/j.msea.2017.01.027.
[79] O.N. Senkov, S.V. Senkova, D.B. Miracle, C. Woodward, Mechanical properties of low-density, refractory multi-principal element alloys of the Cr–Nb–Ti–V–Zr system, Mater. Sci. Eng. A, Struct. Mater.: Prop. Microstruct. Process. 565 (2013) 51–62, https://doi.org/10.1016/j.msea.2012.12.018.
[80] N.D. Stepanov, N.Y. Yurchenko, D.V. Skibin, M.A. Tikhonovsky, G.A. Salishchev, Structure and mechanical properties of the $AlCr_xNbTiV$ ($x = 0, 0.5, 1, 1.5$) high-entropy alloys, J. Alloys Compd. 652 (2015) 266–280, https://doi.org/10.1016/j.jallcom.2015.08.224.
[81] Y. Ma, Q. Wang, B.B. Jiang, C.L. Li, J.M. Hao, X.N. Li, C. Dong, T.G. Nieh, Controlled formation of coherent cuboidal nanoprecipitates in body-centered cubic high-entropy alloys based on $Al_2(Ni,Co,Fe,Cr)_{14}$ compositions, Acta Mater. 147 (2018) 213–225, https://doi.org/10.1016/j.actamat.2018.01.050.
[82] O.N. Senkov, J.K. Jensen, A.L. Pilchak, D.B. Miracle, H.L. Fraser, Compositional variation effects on the microstructure and properties of a refractory high-entropy superalloy $AlMo_{0.5}NbTa_{0.5}TiZr$, Mater. Des. 139 (2018) 498–511, https://doi.org/10.1016/j.matdes.2017.11.033.
[83] Y. Deng, C.C. Tasan, K.G. Pradeep, H. Springer, A. Kostka, D. Raabe, Design of a twinning-induced plasticity high-entropy alloy, Acta Mater. 94 (2015) 124–133, https://doi.org/10.1016/j.actamat.2015.04.014.
[84] Z. Li, K.G. Pradeep, Y. Deng, D. Raabe, C.C. Tasan, Metastable high-entropy dual-phase alloys overcome the strength–ductility trade-off, Nature 534 (2016) 227.
[85] Z. Li, C.C. Tasan, K.G. Pradeep, D. Raabe, A TRIP-assisted dual-phase high-entropy alloy: grain size and phase fraction effects on deformation behavior, Acta Mater. 131 (2017) 323–335, https://doi.org/10.1016/j.actamat.2017.03.069.
[86] L. Lilensten, J.-P. Couzinie, J. Bourgon, L. Perriere, G. Dirras, F. Prima, I. Guillot, Design and tensile properties of a bcc Ti-rich high-entropy alloy with transformation-induced plasticity, Mater. Res. Lett. 5 (2017) 110–116, https://doi.org/10.1080/21663831.2016.1221861.
[87] H. Huang, Y. Wu, J. He, H. Wang, X. Liu, K. An, W. Wu, Z. Lu, Phase-transformation ductilization of brittle high-entropy alloys via metastability engineering, Adv. Mater. 29 (2017) 1701678, https://doi.org/10.1002/adma.201701678.
[88] M. Morinaga, N. Yukawa, T. Maya, K. Sone, H. Adachi, Theoretical design of titanium alloys, in: Sixth World Conference on Titanium. III, 1988, pp. 1601–1606.
[89] M. Abdel-Hady, K. Hinoshita, M. Morinaga, General approach to phase stability and elastic properties of β-type Ti-alloys using electronic parameters, Scr. Mater. 55 (2006) 477–480, https://doi.org/10.1016/j.scriptamat.2006.04.022.
[90] O.N. Senkov, J.D. Miller, D.B. Miracle, C. Woodward, Accelerated exploration of multi-principal element alloys with solid solution phases, Nat. Commun. 6 (2015) 6529, https://doi.org/10.1038/ncomms7529.

[91] O.N. Senkov, J.D. Miller, D.B. Miracle, C. Woodward, Accelerated exploration of multi-principal element alloys for structural applications, Calphad-Comput. Coupl. Phase Diagrams Thermochem. 50 (2015) 32–48, https://doi.org/10.1016/j.calphad.2015.04.009.
[92] D. Miracle, B. Majumdar, K. Wertz, S. Gorsse, New strategies and tests to accelerate discovery and development of multi-principal element structural alloys, Scr. Mater. 127 (2017) 195–200, https://doi.org/10.1016/j.scriptamat.2016.08.001.
[93] S. Vives, P. Bellanger, S. Gorsse, C. Wei, Q. Zhang, J.-C. Zhao, Combinatorial approach based on interdiffusion experiments for the design of thermoelectrics: application to the Mg-2(Si,Sn) alloys, Chem. Mater. 26 (2014) 4334–4337, https://doi.org/10.1021/cm502413t.
[94] J.C. Zhao, Combinatorial approaches as effective tools in the study of phase diagrams and composition-structure-property relationships, Prog. Mater. Sci. 51 (2006) 557–631, https://doi.org/10.1016/j.pmatsci.2005.10.001.
[95] K.N. Wertz, J.D. Miller, O.N. Senkov, Toward multi-principal component alloy discovery: assessment of CALPHAD thermodynamic databases for prediction of novel ternary alloy systems, J. Mater. Res. (2018) 1–14, https://doi.org/10.1557/jmr.2018.61.
[96] S. Naka, T. Khan, Designing novel multiconstituent intermetallics: contribution of modern alloy theory in developing engineered materials, J. Phase Equilib. 18 (1997) 635, https://doi.org/10.1007/BF02665823.
[97] Z. Chen, I. Jones, Sublattice occupancy in 3 Ti–Al–Mo B2 phases, Scr. Metall. Mater. 32 (1995) 553–557, https://doi.org/10.1016/0956-716X(95)90836-9.
[98] T. Sikora, G. Hug, M. Jaouen, A.M. Flank, EXAFS study of the local atomic order in Ti(2)AlX (X=Nb,Mo) B2 intermetallic compounds, J. Phys. IV 6 (1996) 15–20, https://doi.org/10.1051/jp4:1996203.
[99] S. Huang, E. Hall, The effects of Cr additions to binary TiAl-base alloys, Metall. Trans. A, Phys. Metall. Mater. Sci. 22 (1991) 2619–2627, https://doi.org/10.1007/BF02851355.
[100] D. Banerjee, The intermetallic Ti_2AlNb, Prog. Mater. Sci. 42 (1997) 135–158, https://doi.org/10.1016/S0079-6425(97)00012-1.
[101] A. Pathak, A.K. Singh, A first principles study of Ti_2AlNb intermetallic, Solid State Commun. 204 (2015) 9–15, https://doi.org/10.1016/j.ssc.2014.12.002.
[102] K. Das, S. Das, Order–disorder transformation of the body centered cubic phase in the Ti–Al–X (X=Ta, Nb, or Mo) system, J. Mater. Sci. 38 (2003) 3995–4002, https://doi.org/10.1023/A:1026262616194.
[103] S. Das, J. Perepezko, Ternary phase development in the Ti–Al–Ta system, Scr. Metall. Mater. 25 (1991) 1193–1198, https://doi.org/10.1016/0956-716X(91)90527-8.
[104] M. Weaver, M. Kaufman, Phase-relationships and transformations in the ternary aluminum–titanium–tantalum system, Acta Metall. Mater. 43 (1995) 2625–2640, https://doi.org/10.1016/0956-7151(94)00468-W.
[105] P. Villars, A 3-dimensional stability diagram for 998 binary AB intermetallic compounds, J. Less-Common Met. 92 (1983) 215–238, https://doi.org/10.1016/0022-5088(83)90489-7.
[106] D. Pettifor, Structure maps for pseudobinary and ternary phases, Mater. Sci. Technol. 4 (1988) 675–691, https://doi.org/10.1179/mst.1988.4.8.675.
[107] Y. Harada, M. Morinaga, J. Saito, Y. Takagi, New crystal structure maps for intermetallic compounds, J. Phys. Condens. Matter 9 (1997) 8011–8030, https://doi.org/10.1088/0953-8984/9/38/008.
[108] S. Curtarolo, D. Morgan, G. Ceder, Accuracy of ab initio methods in predicting the crystal structures of metals: a review of 80 binary alloys, Calphad-Comput. Coupl. Phase Diagrams Thermochem. 29 (2005) 163–211, https://doi.org/10.1016/j.calphad.2005.01.002.
[109] N.Y. Chen, W.C. Lu, R.L. Chen, P. Qin, P. Villars, Regularities of formation of ternary intermetallic compounds – Part 1. Ternary intermetallic compounds between nontransition elements, J. Alloys Compd. 289 (1999) 120–125.
[110] S. Curtarolo, D. Morgan, K. Persson, J. Rodgers, G. Ceder, Predicting crystal structures with data mining of quantum calculations, Phys. Rev. Lett. 91 (2003) 135503, https://doi.org/10.1103/PhysRevLett.91.135503.
[111] E. Menou, I. Toda-Caraballo, P.E.J. Rivera-Diaz-del-Castillo, C. Pineau, E. Bertrand, G. Ramstein, F. Tancret, Evolutionary design of strong and stable high-entropy alloys using multi-objective optimisation based on physical models, statistics and thermodynamics, Mater. Des. 143 (2018) 185–195, https://doi.org/10.1016/j.matdes.2018.01.045.
[112] S. Curtarolo, W. Setyawan, S. Wang, J. Xue, K. Yang, R.H. Taylor, L.J. Nelson, G.L.W. Hart, S. Sanvito, M. Buongiorno-Nardelli, N. Mingo, O. Levy, AFLOWLIB.ORG: A distributed materials properties repository from high-throughput ab initio calculations, Comput. Mater. Sci. 58 (2012) 227–235, https://doi.org/10.1016/j.commatsci.2012.02.002.
[113] A. Jain, G. Hautier, C.J. Moore, S.P. Ong, C.C. Fischer, T. Mueller, K.A. Persson, G. Ceder, A high-throughput infrastructure for density functional theory calculations, Comput. Mater. Sci. 50 (2011) 2295–2310, https://doi.org/10.1016/j.commatsci.2011.02.023.
[114] D.D. Landis, J.S. Hummelshoj, S. Nestorov, J. Greeley, M. Dulak, T. Bligaard, J.K. Norskov, K.W. Jacobsen, The computational materials repository, Comput. Sci. Eng. 14 (2012) 51–57, https://doi.org/10.1109/MCSE.2012.16.
[115] M. Klintenberg, The Electronic Structure Project, n.d., http://gurka.fysik.uu.se/esp-fs/.
[116] S. Kirklin, J.E. Saal, B. Meredig, A. Thompson, J.W. Doak, M. Aykol, S. Ruehl, C. Wolverton, The Open Quantum Materials Database (OQMD): assessing the accuracy of DFT formation energies, Npj Comput. Mater. 1 (2015), https://doi.org/10.1038/npjcompumats.2015.10, UNSP 15010.
[117] M. Mihalkovic, M. Widom, Ab initio calculations of cohesive energies of Fe-based glass-forming alloys, Phys. Rev. B 70 (2004) 144107, https://doi.org/10.1103/PhysRevB.70.144107.